Inorganic Chemistry

pubs.acs.org/IC Article

Effect of Substituents on the Crystal Structures, Optical Properties, and Catalytic Activity of Homoleptic Zn(II) and Cd(II) *β*-oxodithioester Complexes

Chote Lal Yadav, Anamika, Gunjan Rajput, Kamlesh Kumar, Michael G. B. Drew, and Nanhai Singh*

Cite This: https://dx.doi.org/10.1021/acs.inorgchem.0c01195 Read Online

ACCESS | Metrics & More | Article Recommendations | SI Supporting Information

ABSTRACT: Five novel zinc(II) and cadmium(II) *β*-oxodithioester complexes, $[Zn(\mathbf{L1})_2]$ (**1**), $[Zn(\mathbf{L2})_2]_n$ (**2**), $[Zn(\mathbf{L3})_2]_n$ (**3**) $[Cd(\mathbf{L1})_2]_n$ (**4**), $[Cd(\mathbf{L2})_2]_n$ (**5**), with *β*-oxodithioester ligands, where **L1** = 3-(methylthio)-1-(thiophen-2-yl)-3-thioxoprop-1-en-1-olate, **L2** = 3-(methylthio)-1-(pyridin-3-yl)-3-thioxoprop-1-en-1-olate, and **L3** = 3-(methylthio)-1-(pyridin-4-yl)-3-thioxoprop-1-en-1-olate, were synthesized and characterized by elemental analysis, IR, UV−vis, and NMR spectroscopy (^{1}H and ^{13}C{^{1}H}). The solid-state structures of all complexes were ascertained by single-crystal X-ray crystallography. The *β*-oxodithioester ligands are bonded to Zn(II)/Cd(II) metal ions in an O^S and N chelating/chelating−bridging fashion leading to the formation of 1D (in **2**−**4**) and 2D (in **5**) coordination polymeric structures, but complex **1** was obtained as a discrete tetrahedral molecule. Complex **4** crystallizes in the *C*2 chiral space group and has been studied using circular dichroism (CD) spectroscopy. The multidimensional assemblies in these complexes are stabilized by many important noncovalent C−H···*π* ($ZnOSC_3$, chelate), *π*···*π*, C−H···*π*, and H···H interactions. The catalytic activities of **1**−**5** in reactions involving C−C and C−O bond formation have been studied, and the results indicated that complex **3** can be efficiently utilized as a heterogeneous bifunctional catalyst for the Knoevenagel condensation and multicomponent reactions to develop biologically important organic molecules. The luminescent properties of complexes were also studied. Interestingly, zinc complexes **1**−**3** showed strong lumniscent emission in the solid state, whereas cadmium complexes **4** and **5** exhibited bright luminescent emission in the solution phase. The semiconducting behavior of the complexes was studied by solid-state diffuse reflectance spectra (DRS), which showed optical band gaps in the range of 2.49−2.62 eV.

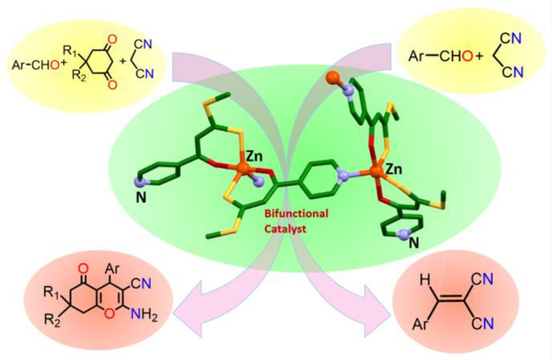

INTRODUCTION

Coordination polymers (CPs) derived from transition-metal ions and organic ligands have received considerable attention in recent years due to their multifaceted chemistry, intriguing structural features, and photophysical properties as well as their diverse applications in catalysis, adsorption, and conductivity.[1−9] In general, the properties of coordination polymers are greatly affected by their structures, the nature of the metal ions, and the steric and electronic properties of functional groups attached to the organic linkers.[1−6] The porous nature and larger surface area of CPs along with open Lewis acid sites make them suitable catalysts for several organic reactions such as Knoevenagel condensation,[8] cyanation,[9a] Strecker reaction,[9b] aldol condensation,[9c] transesterification,[9d] reactions of epoxide,[9e] hydrogenation,[9f] oxidation,[9g] Friedel−Crafts alkylation,[9h] the Henry reaction,[9i] Suzuki−Miyaura cross-coupling,[9j] and Michael addition.[9k] However, there have been only a few studies of organic transformation reactions catalyzed by bifunctional CPs: i.e., those having acidic and basic sites within their architectures.[10]

In the majority of complexes reported so far, the coordination sphere of the metal is closely controlled through the use of bridging/chelating/monodentate ligands containing N/O/S donor atoms.[1−5] Dithioesters have found applications in ionic resins for the separation of transition-metal ions,[11] for Ag^+-selective membrane electrodes,[12] and as hair-growing agents in combination with zinc.[13] The *β*-oxodithioesters are strongly O^S-chelating ligands and have been utilized to synthesize homo- and heteroleptic complexes with several transition metals, yielding a stable delocalized six-membered ring about the metal center.[14,15] The metal complexes of organosulfur ligands including those of *β*-oxodithioesters have served as catalysts in a variety of organic transformation

Received: April 22, 2020

Scheme 1. Synthesis of Complexes 1−5 from KL1−KL3 and Metal Salts

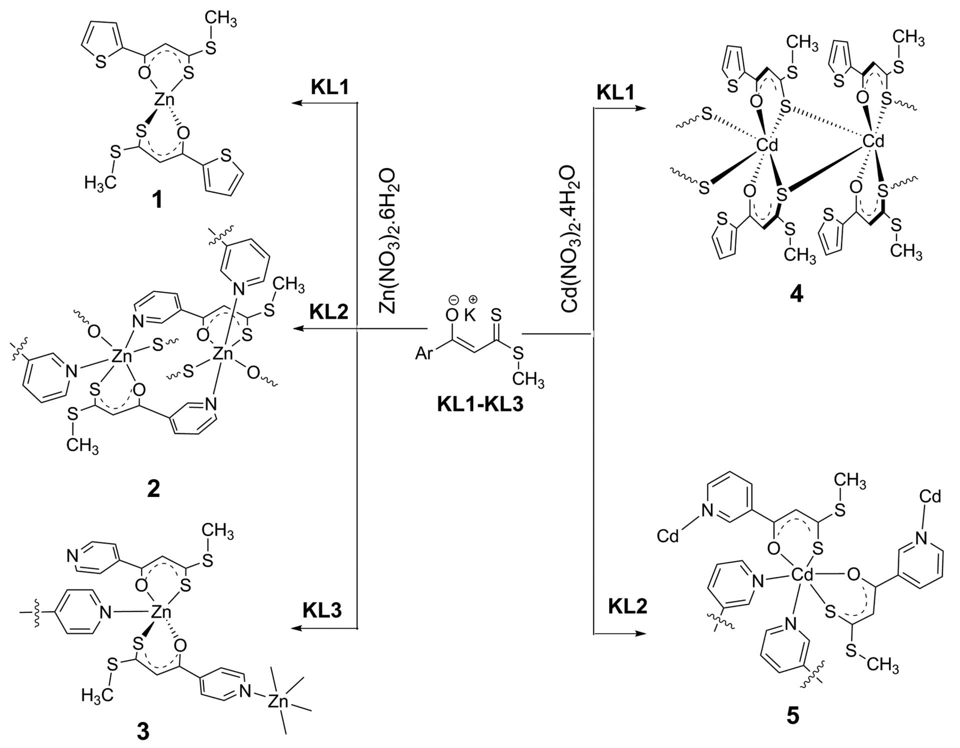

reactions[16] and also exhibited biological properties such as antileishmanial and anticancer activities.[15] Intriguing coordination polymeric structures and photoluminescence properties of Tl(I) *β*-oxodithioester complexes displaying varied polymeric structures have also been described.[17] Recently, a chiral compound was obtained via spontaneous resolution and chirality induction (using chiral inducers) in a discrete tetrahedral Zn(II) complex containing an achiral *β*-oxodithioester ligand.[18] Despite their synthetic versatility and practical applicability, the chemistry and photophysical properties of group 12 metal (Zn, Cd, Hg) complexes with *β*-oxodithioester ligands have been much less explored.[18,19]

In this contribution, the synthesis, crystal structures, and optical, conducting, and catalytic properties of homoleptic Zn(II) and Cd(II) complexes **1**−**5** with functionalized *β*-oxodithioester ligands (Scheme 1) are presented. The important aspect of undertaking this work is to study the effect of the steric and electronic aspects of substituents on the *β*-oxodithioester backbone on the structure and luminescent and semiconducting properties of the complexes. Also, the catalytic activities of the complexes in the Knoevenagel condensation and multicomponent reactions are explored. The following points provided the main impetus for undertaking this work. (i) It is critical to make methodical changes to the ligand environments in order to map out both the structural features and photophysical properties of the complexes. Accordingly, 3-pyridyl, 4-pyridyl, and 2-thienyl groups have been incorporated into the *β*-oxodithioester framework to influence the electronic and steric properties of the ligands and hence the complexes. (ii) Zn(II) and Cd(II) metals with a d^{10} configuration display no stereochemical preferences arising from the ligand field stabilization effects. Therefore, they may show a variety of coordination numbers and stereochemical arrangements on the basis of the interplay of electrostatic forces, covalent bonds, and size factors. Usually they have a tetrahedral/octahedral geometry. (iii) The *β*-oxodithioesters having both hard "O" and distinctly soft "S" donor atoms may display chelating/bridging behavior toward Cd(II), a soft metal ion, and Zn(II) in the border of hard and soft Lewis acids. The highly electronegative oxygen has small p orbitals, whereas the large and less electronegative sulfur has more diffuse d orbitals that may facilitate better metal−ligand overlapping and hence electron delocalization in the molecule. Furthermore, because of the differences in these properties, the HOMO−LUMO gap may be substantially modified, thereby influencing the luminescent characteristics of the complexes. (iv) The additional donor atoms on the substituents can be involved in bonding to the metal centers on adjacent molecules to generate extended polymeric structures and to sustain multidimensional supramolecular networks through secondary noncovalent interactions, thereby tuning the solid-state emission properties. Also, the lone pair of pyridyl(N) may enhance the electron conjugation within the extended rigid polymeric structure and therefore the solid-state emission properties of the complexes.

■ EXPERIMENTAL SECTION

General Methods and Materials. All reactions were carried out in the open and at room temperature unless specifically mentioned. The solvents were purified by standard procedures and, where necessary, dried before use.[20] All of the commercially available reagents of analytical grade were purchased from Sigma-Aldrich, Spectrochem, S. D. Fine Chemicals, or Avra and were used as received without further purification. Melting points of the complexes were determined in open capillaries with a Gallenkamp apparatus and are uncorrected. FTIR spectra in the 4000−400 cm^{-1} region were recorded as KBr disks using a PerkinElmer FTIR spectrophotometer. Elemental analyses (C, H, and N) were performed with an Elementar Vario EL III Carlo Erba 1108 elemental analyzer. ^1H and $^{13}C\{^1H\}$ NMR spectra were obtained in $CDCl_3$/DMSO-d_6 on a JEOL ECZ 500 MHz FT NMR/Bruker 400 MHz spectrometer.[17] Tetrmethylsilane (TMS) was used as an internal standard for recording NMR spectra. CD spectra were collected on a JASCO J-815 spectrophotometer. UV−visible absorption spectra in solution (DMSO) and the solid state were obtained on a Shimadzu UV-1800 instrument and a Harrick Praying Mantis accessory on a Shimadzu UV-3600 instrument, whereas emission spectra were recorded on Fluorolog Horiba Jobin Yvon spectrophotometers. Powder X-ray diffraction (PXRD) patterns were collected using a Rigaku MiniFlex-600W system with Cu Kα radiation (λ = 1.54056 Å), in which the X-ray tube was operated at a voltage of 40 kV, a current of 20 mA, and an angular range 2θ = 5−50° with a scan rate of 2° min^{-1} and a step size of 0.02°.

Synthesis of the Ligands HL1−HL3 and Their Potassium Salts KL1−KL3. The ligands, methyl 3-hydroxy-3-(2-thienyl)-2-propenedithioate (**HL1**), methyl 3-hydroxy-3-(3-pyridyl)-2-propenedithioate (**HL2**), and methyl 3-hydroxy-3-(4-pyridyl)-2-propenedithioate (**HL3**) and their potassium salts **KL1−KL3** were prepared by following the procedure previously reported (Scheme 2).[17] In the general procedure, an acetyl derivative (10.0 mmol) was added dropwise to a solution of NaH (0.6 g, 25 mmol) in a DMF/hexane mixture (4/1; 20 mL) with constant stirring under an N_2 atmosphere. After the mixture was stirred for 1 h in an ice bath, a solution of dimethyltrithiocarbonate (TTC)[21] (1.38 g, 10 mmol) was added slowly and the reaction mixture was further stirred for 10 h at room temperature. Excess NaH was neutralized by adding 0.1 M HCl (50 mL), and the product was extracted with dichloromethane (3 × 50 mL). The dichloromethane solution was collected, washed with water and brine solution, and dried over anhydrous Na_2SO_4. The crude product was further purified by silica gel (100−200 mesh) chromatography using hexane as the eluent, resulting in **HL1−HL3** as yellow solids (characterization data and NMR and FTIR spectra are given in sections S1−S3 in the Supporting Information). Further, the potassium salts of the ligands **KL1−KL3** were obtained by refluxing solutions of **HL1−HL3** (1.0 mmol) with solid K_2CO_3 (0.21 g, 1.5 mmol) in acetone (10 mL) for 4−5 h with constant stirring. The solution was cooled and filtered, and the filtrate was dried using a rotary evaporator to yield **KL1−KL3** as orange solid products.

Scheme 2. Synthesis of the Ligands HL1−HL3 and Their Potassium Salts KL1−KL3

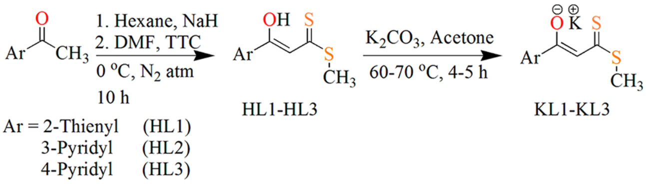

Synthesis and Characterization of Complexes 1−5. *[Bis{3-(methylthio)-1-(thiophen-2-yl)-3-thioxoprop-1-en-1-olato-S^O}-zinc(II)] (**1**).* A solution of $Zn(NO_3)_2{\cdot}6H_2O$ (0.148 g, 0.5 mmol) in 10 mL of methanol/water (80/20) was added dropwise to a 10 mL methanolic solution of the potassium salt of the ligand **KL1** (0.254 g, 1 mmol) at room temperature with stirring. The reaction mixture was further stirred for 2 h. The yellow solid thus formed was filtered, washed with methanol, and dried in air. Pale yellow needle-shaped crystals of product were obtained from a DMF solution of the compound within 2−3 weeks. Empirical formula: $[Zn(L1)_2]$. Yield: 0.45 g, 91%. Mp: 216−220 °C. ^{1}H NMR (500 MHz, DMSO-d_6, ppm): δ 7.95 (d, J = 3.5 Hz, 1H, $-C_4H_3S$), 7.91 (d, J = 5.0 Hz, 1H, $-C_4H_3S$), 7.20 (t, 1H, $-C_4H_3S$), 6.99 (s, 1H, $-CH{=}C(S)-$), 2.55 (s, 3H, $-SCH_3$). $^{13}C\{^1H\}$ NMR (125 MHz, DMSO-d_6, ppm): δ 189.3 ($=C-S$), 172.6 ($-C{=}O$), 153.3, 146.9, 116.2, 112.8 ($-C_4H_3S$), 107.6 ($=CH-C(S)-$), 16.6 ($-SCH_3$). IR (KBr, cm^{-1}): 1572 ($\nu_{C=O}$), 1524 ($\nu_{C=C}$), 1101 (ν_{C-S}). Anal. Calcd for $C_{16}H_{14}O_2S_6Zn$ (496.0): C, 38.74; H, 2.84. Found: C, 38.61; H, 3.05. UV−vis: DMSO, λ_{max} (nm), ε (M^{-1} cm^{-1}) 410 (8.19 × 10^4), 315 (2.18 × 10^4); Nujol, λ_{max} (nm) 325, 430.

*Poly[bis{μ_2-3-(methylthio)-1-(pyridin-3-yl)-3-thioxoprop-1-en-1-olato-κ^3S^O:N}zinc(II)] (**2**).* Complex **2** was prepared following the procedure used in the synthesis of complex **1** from **KL2** (0.249 g, 1 mmol) and $Zn(NO_3)_2{\cdot}6H_2O$ (0.148 g, 0.5 mmol). A yellow precipitate was obtained in the reaction, and brown needle-shaped crystals of **2** suitable for X-ray studies were obtained from DMF solution of the compound within 2−3 weeks. Empirical formula: $[Zn(L2)_2]_n$. Yield: 0.41 g, 85%. Mp: 207−212 °C. ^{1}H NMR (500 MHz, DMSO-d_6, ppm): δ 9.11 (s, 1H, $-C_5H_4N$), 8.33 (d, J = 4.0 Hz, 1H, $-C_5H_4N$), 8.29 (d, J = 7.5 Hz, 1H, $-C_5H_4N$), 7.54 (dd, J = 7.5, 4.0 Hz, 1H, $-C_5H_4N$), 7.04 (s, 1H, $-CH{=}C(S)-$), 2.58 (s, 3H, $-SCH_3$). $^{13}C\{^1H\}$ NMR (125 MHz, DMSO-d_6, ppm): δ 193.3 ($=C-S$), 181.9 ($-C{=}O$), 152.1, 148.5, 135.3, 135.0, 123.8 ($-C_5H_4N$), 108.9 ($=CH-C(S)-$), 16.9 ($-SCH_3$). IR (KBr, cm^{-1}): 1580 ($\nu_{C=O}$), 1468 ($\nu_{C=C}$), 1118 (ν_{C-S}). Anal. Calcd for $C_{18}H_{16}N_2O_2S_4Zn$ (485.94): C, 44.49; H, 3.32; N, 5.76. Found: C, 44.25; H, 3.37; N, 5.53. UV−vis: DMSO, λ_{max} (nm), ε (M^{-1} cm^{-1}) 400 (8.49 × 10^4), 315 (1.94 × 10^4); Nujol, λ_{max} (nm) 335, 400.

*Poly[{3-(methylthio)-1-(pyridin-4-yl)-3-thioxoprop-1-en-1-olato}{μ_2-3-(methylthio)-1-(pyridin-4-yl)-3-thioxoprop-1-en-1-olato-κ^3S^O:N}zinc(II)] (**3**).* Complex **3** was prepared following the procedure used in the synthesis of complex **1** from **KL3** (0.249 g, 1 mmol) and $Zn(NO_3)_2{\cdot}6H_2O$ (0.148 g, 0.5 mmol). A yellow precipitate was obtained in the reaction, and brown needle-shaped crystals of **3** suitable for X-ray studies were obtained from a DMF solution of the compound within 2−3 weeks. Empirical formula: $[Zn(\mathbf{L3})_2]_n$. Yield: 0.43 g, 89%. Mp: 214−218 °C. ^{1}H NMR (500 MHz, DMSO-d_6, ppm): δ 8.73 (s, 2H, $-C_5H_4N$), 7.82 (s, 2H, $-C_5H_4N$), 7.04 (s, 1H, $-CH{=}C(S)-$), 2.58 (s, 3H, $-SCH_3$). $^{13}C\{^1H\}$ NMR (125 MHz, DMSO-d_6, ppm): δ 195.7 ($=C-S$), 181.2 ($-C{=}O$), 150.5, 146.9, 121.0 ($-C_5H_4N$), 108.7 ($=CH-C(S)-$), 16.9 ($-SCH_3$). IR (KBr, cm^{-1}): 1571 ($\nu_{C=O}$), 1503 ($\nu_{C=C}$), 1064 (ν_{C-S}). Anal. Calcd for $C_{18}H_{16}N_2O_2S_4Zn$ (485.94): C, 44.49; H, 3.32; N, 5.76. Found: C, 44.32; H, 3.43; N, 5.61. UV−vis: DMSO, λ_{max} (nm), ε (M^{-1} cm^{-1}) 415 (8.46 × 10^4), 315 (2.02 × 10^4); Nujol, λ_{max} (nm) 335, 400.

*Poly[bis{μ_2-3-(methylthio)-1-(thiophen-2-yl)-3-thioxoprop-1-en-1-olato-κ^3S^O:S}cadmium(II)] (**4**).* A solution of $Cd(NO_3)_2{\cdot}4H_2O$ (0.154 g, 0.5 mmol) in 10 mL of methanol/water (80/20) was added dropwise to a 10 mL methanolic solution of the potassium salt of the ligand **KL1** (0.254 g, 1 mmol) at room temperature with stirring. The reaction mixture was further stirred for 2 h. The yellow solid thus formed was filtered, washed with methanol, and dried in air. Pale yellow needle-shaped crystals of **4** suitable for X-ray studies were obtained from a DMF solution of the compound within 2−3 weeks. Empirical formula: $[Cd(\mathbf{L1})_2]_n$. Yield: 0.40 g, 73%. Mp: 172−175 °C. ^{1}H NMR (400 MHz, DMSO-d_6, ppm): δ 7.79 (d, J = 4.8 Hz, 1H, $-C_4H_3S$), 7.76 (d, J = 3.2 Hz, 1H, $-C_4H_3S$), 7.79 (t, 1H, $-C_4H_3S$), 6.87 (s, 1H, $-CH{=}C(S)-$), 2.47 (s, 3H, $-SCH_3$). $^{13}C\{^1H\}$ NMR (100 MHz, DMSO-d_6, ppm): δ 187.8 ($=C-S$), 178.1 ($-C{=}O$), 148.0, 132.5, 129.0, 128.3 ($-C_4H_3S$), 109.1 ($=CH-C(S)-$), 17.14 ($-SCH_3$). IR (KBr, cm^{-1}): 1547 ($\nu_{C=O}$), 1515 ($\nu_{C=C}$), 1065 (ν_{C-S}). Anal. Calcd for $C_{16}H_{14}O_2S_6Cd$ (543.03): C, 35.39; H, 2.60. Found: C, 35.18; H, 2.70. UV−vis: DMSO, λ_{max} (nm), ε (M^{-1} cm^{-1}) 410 (8.54 × 10^4), 315 (2.39 × 10^4); Nujol, λ_{max} (nm) 325, 400.

*Poly[bis{μ_2-3-(methylthio)-1-(pyridin-3-yl)-3-thioxoprop-1-en-1-olato-κ^3S^O:N}cadmium(II)] (**5**).* Complex **5** was prepared following the procedure used in the synthesis of complex **4** from **KL2** (0.249 g, 1 mmol) and $Cd(NO_3)_2{\cdot}4H_2O$ (0.154 g, 0.5 mmol). A yellow precipitate was obtained in the reaction, and brown rectangular-shaped crystals of **5** suitable for X-ray studies were obtained from a DMF solution of the compound within 2−3 weeks. Empirical formula: $[Cd(\mathbf{L2})_2]_n$. Yield: 0.42 g, 79%. Mp: 195−198 °C. ^{1}H NMR (500 MHz, DMSO-d_6, ppm): δ 9.01 (s, 1H, $-C_6H_4N$), 8.67 (d, J = 6.0 Hz, 1H, $-C_5H_4N$), 8.16 (d, J = 8.5 Hz, 1H, $-C_5H_4N$), 7.46−7.44 (m, 1H, $-C_5H_4N$), 6.87 (s, 1H, $-CH{=}C(S)-$), 2.53 (s, 3H, $-SCH_3$). $^{13}C\{^1H\}$ NMR (125 MHz DMSO-d_6, ppm): δ 191.4 ($=C-S$), 183.0 ($-C{=}O$), 151.5, 148.5, 136.3, 134.9, 123.5 ($-C_5H_4N$), 109.7 ($=CH-C(S)-$), 17.3 ($-SCH_3$). IR (KBr, cm^{-1}): 1596 ($\nu_{C=O}$), 1515 ($\nu_{C=C}$), 1065 (ν_{C-S}). Anal. Calcd for $C_{18}H_{16}N_2O_2S_4Cd$ (532.97): C, 40.56; H, 3.03; N, 5.26. Found: C, 40.48; H, 2.85; N,

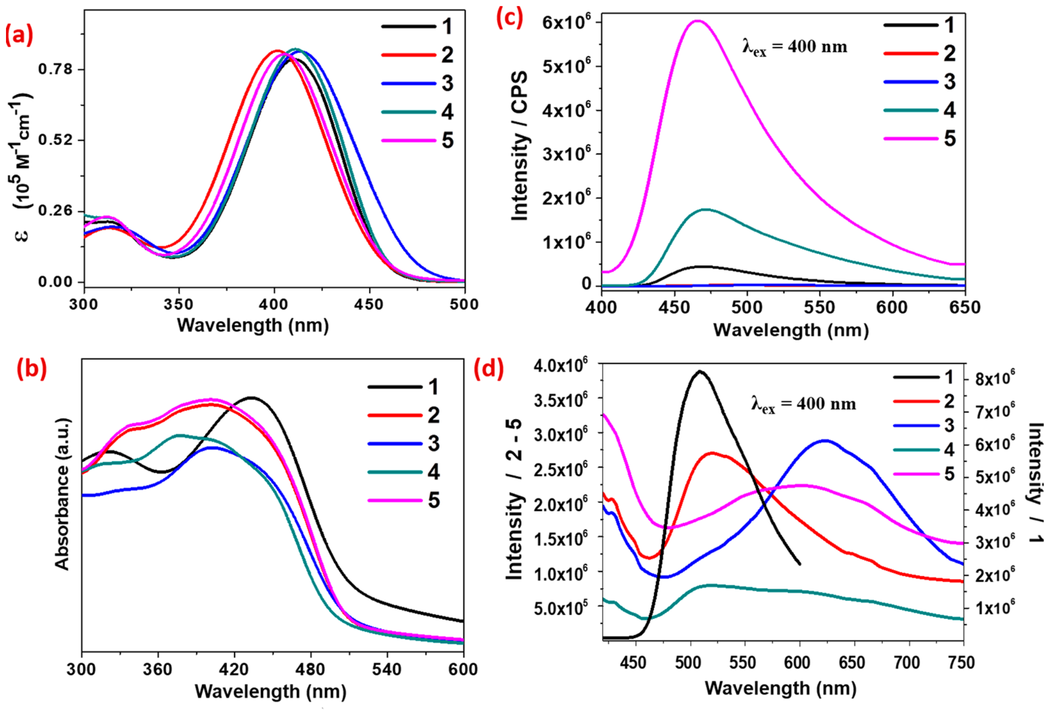

Figure 1. (a) UV−vis absorption in DMSO solution, (b) solid-state UV−vis absorption in Nujol mull, (c) fluorescence spectra in DMSO solution, and (d) solid-state fluorescence spectra of complexes **1**−**5**.

4.96. UV−vis: DMSO, λ_{max} (nm), ε (M^{-1} cm^{-1}) 405 (8.41×10^4), 315 (2.39×10^4); Nujol, λ_{max} (nm) 335, 400.

Procedure for the Knoevenagel Condensation Reactions. Knoevenagel condensation reactions were performed according to the reported procedure.[8,10] In a typical reaction, a double-neck round-bottom flask was charged with benzaldehyde (0.107 g, 1.0 mmol), malononitrile (0.066 g, 1.0 mmol), and catalyst **3** (0.024 g, 5 mol %). Methanol (5 mL) was placed in the reaction flask, and the reaction mixture was stirred at 60 °C for 1 h. The progress of the reaction was monitored by thin-layer chromatography (TLC), and the reaction mixture was filtered after 1 h to separate the catalyst. The solvent was removed *in vacuo* from the clear filtrate, giving the crude product, which was further purified by silica gel column chromatography using 9/1 hexanes/EtOAc as the eluent. The final product was obtained as a white solid that was further characterized by NMR spectral analysis. The isolated yield and characterization data as well as NMR spectra of the Knoevenagel condensation products are given in sections S7 and S8 in the Supporting Information.

Procedure for One-Pot Multicomponent Reactions (Synthesis of 2-Amino-4*H*-chromene Derivatives). In a typical reaction, a double-neck round-bottom flask was charged with benzaldehyde (0.107 g, 1.0 mmol), malononitrile (0.066 g, 1.0 mmol), cyclohexane-1,3-dione (0.112 g, 1.0 mmol), and catalyst **3** (0.024 g, 5 mol %). Ethanol (10 mL) was placed in the reaction flask, and the reaction mixture was stirred at 80 °C for 1.5 h. The progress of the reaction was monitored by thin-layer chromatography (TLC), and the reaction mixture was filtered after 1.5 h to separate the catalyst. The solvent was removed *in vacuo* from the clear filtrate, giving the crude product, which was further purified by silica gel column chromatography using 1/1 hexanes/EtOAc as the eluent. The product was obtained as an off-white solid which was further characterized by NMR spectral analysis. The isolated yield and characterization data as well as NMR spectra of 2-amino-4*H*-chromene derivatives are given in sections S9 and S10 in the Supporting Information.

Theoretical Calculations. Single-point calculations were carried out using the Gaussian 03 program.[22] Structures were optimized using the B3LYP density functional together with the basis sets LANL2DZ for Zn and Cd, 6-31+G* for S, N, and O, and 6-31G for the remaining atoms. Starting models were taken from the crystal structures but with hydrogen atoms given theoretical normalized positions.

X-ray Structure Determinations. Single-crystal X-ray diffraction data for complexes **1**, **2**, and **4** were collected on an Oxford Diffraction X-Calibur CCD diffractometer using Mo Kα radiation (λ = 0.71073 Å) at 150 K; those of **3** and **5** were collected on a Bruker SMART CCD diffractometer with graphite-monochromated Mo Kα radiation at 100 K. Data reduction for **1**, **2**, and **4** was carried out using the CrysAlis program[23] and that for **3** and **5** using Bruker SAINT.[24] All structures were solved by direct methods using SHELXS-97[25] and refined on F^2 by a full-matrix least-squares technique using SHELXL2016-6.[26] Non-hydrogen atoms were refined anisotropically, and hydrogen atoms were geometrically fixed with thermal parameters equivalent to 1.2 times that of the atom to which they were bonded. In complex **1** the sulfur atom in the thienyl ring is disordered over two positions. In complex **4**, the thienyl ring is more severely disordered with four different arrangements in which there are two different orientations of the five-membered ring and then two different positions of the sulfur atom in each. Diagrams for complexes **1**−**5** were prepared using DIAMOND[27a] and Mercury[27b] software. Crystallographic data for **1**−**5** were deposited at the Cambridge Crystallographic Data Centre with reference numbers CCDC 1983320, 1983319, 1998352, 1983318, and 1983321.

RESULTS AND DISCUSSION

Synthesis and Spectral Characterization of Complexes 1−5. The reactions of the potassium salts of the β-oxodithioester ligands **KL1**−**KL3** with methanol/water (80/20, v/v) solutions of Zn(NO$_3$)$_2$·6H$_2$O and Cd(NO$_3$)$_2$·4H$_2$O in a 2:1 molar ratio resulted in the formation of the homoleptic complexes **1**−**5** in good yield (Scheme 1). All complexes were obtained as air- and moisture-stable pale yellow solids. Zinc complexes are insoluble in water, methanol, ethanol, and acetonitrile and sparingly soluble in dichloromethane, chloroform, and acetone but are soluble in DMF and DMSO. Cadmium complexes are insoluble in common organic solvents but are sparingly soluble in DMF and DMSO. All complexes were fully characterized by elemental analysis, IR, UV−vis, and ^1H and $^{13}C\{^1H\}$ NMR spectral analyses. The monomeric structure of **1** and coordination polymeric structures of **2**−**5** have also been confirmed by single-crystal X-ray crystallography (SCXRD). The homogeneity of the bulk samples of **1**−**5** was ascertained by comparing the experimental PXRD patterns with the respective simulated powder patterns obtained from the single-crystal data. The peak positions of the experimental and simulated PXRD patterns matched well, revealing the phase purity of bulk products (Figure S1 in the Supporting Information). The semiconducting behavior of the complexes has been studied by diffuse reflectance spectra (DRS). All the complexes show luminescent properties in both the solution and solid phase.

In the IR spectra, complexes **1**−**5** display bands at 1596−1547, 1524−1464, and 1118−1027 cm^{-1} for the $\nu_{C=O}$, $\nu_{C=C}$ and ν_{C-S} vibrations, respectively, diagnostic of a coordinated β-oxodithioester ligand.[14,17,18] The free ligands **HL1**−**HL3** show characteristic bands at 1065−1060, 1591−1576, and 1232−1217 cm^{-1} for the ν_{C-OH}, $\nu_{C=C}$ and $\nu_{C=S}$ frequencies, respectively. The decrease in the ν_{C-S} frequency in complexes **1**−**5** in comparison to **HL1**−**HL3** is indicative of coordination via the S atom of the −SCSMe group of the dithioester ligands. In the ^1H NMR spectra of the ligands **HL1**−**HL3**, the signals of the −OH proton signal appear at chemical shift values (δ) of ∼15.0 ppm, and these signals are absent in complexes **1**−**5**. The signal for the vinylic proton in the complexes appeared at δ 6.82−7.04 ppm, remaining unchanged in comparison to the corresponding ligands. The signal for the methyl protons of $-SCH_3$ in the complexes did not show a significant shift and appeared at δ ∼2.50 ppm.

The O^S bidentate mode of binding of ligands with Zn(II)/Cd(II) metal ions is also revealed by $^{13}C\{^1H\}$ NMR spectral studies. In $^{13}C\{^1H\}$ NMR spectra, the resonance for the C−OH carbon in the free ligands is observed at δ 164.3−166.2 ppm, which is shifted downfield by 8−17 ppm in the spectra for the complexes and appeared at δ 172.6−183.0 ppm. This indicates coordination of the metal toa −C═O oxygen and partial double-bond character in the C═O group.[14,17−19] The −C═S carbon located at δ 216.0−219.4 ppm in the free ligand shows an upfield shift and is observed at δ 187.8−195.7 ppm in the complexes, indicating metal−sulfur bonding. These findings are further supported by the crystal structures (*vide infra*). The signal for the vinylic carbon of the ligands is not affected significantly on coordination with metal ions and appeared at δ 107.6−109.7 ppm.

Optical Properties. *Absorption and Emission Spectral Studies.* We have studied the absorption characteristics of the ligands **HL1**−**HL3** and their corresponding complexes **1**−**5** by recording UV−vis spectra in dichloromethane (section S6 in the Supporting Information) and DMSO (Figure 1a) solutions, respectively. The solid-state UV−vis spectra of the complexes have also been recorded (Figure 1b). Absorption spectra of the complexes in solution and the solid state are similar, apart from variations in peak intensity. UV−vis spectra of the ligands **HL1**−**HL3** show absorptions near 290 and 360−400 nm in dichloromethane solution. The DMSO solutions of complexes **1**−**5** display bands near 315 nm (ε = $(1.94-2.39) \times 10^4\ M^{-1}\ cm^{-1}$) and 400−415 nm ($\varepsilon$ = $(8.19-8.54) \times 10^4\ M^{-1}\ cm^{-1}$) and are assigned to slightly metal perturbed ligand-centered and intraligand charge transfer (ILCT) transitions, respectively. The complexes in the solid state showed similar transitions at 325−335 and 400−430 nm.[4a,b,f]

In emission spectral studies the Zn(II) complexes **1**−**3** exhibited strong emission bands in comparison to Cd(II) complexes **4** and **5** in the solid state, whereas the latter showed strong fluorescence in DMSO solution. The cadmium complexes **4** and **5** upon excitation at 400 nm in DMSO solution show unstructured strong emission bands at $\lambda_{emis}{}^{max}$ 465−475 nm (Figure 1c) that emanate from the intraligand charge transfer (ILCT) and metal-perturbed ILCT states.[4a,b] However, the zinc complexes **1**−**3** are only weakly fluorescent in solution (Figure 1c). All complexes on excitation at 400 nm in the solid phase exhibit $\lambda_{emis}{}^{max}$ at 510−625 nm at room temperature with a noticeable red shift in comparison to the values in solution (Figure 1d), thus indicating that the luminescent behavior is slightly different in the two media. It is worth noting that despite a close homology in the chemistry of zinc and cadmium, the latter exhibits a coordination number of 6 more frequently than zinc owing to its larger size. The difference observed in the luminescent characteristics of the zinc(II) and cadmium(II) complexes may be attributed to the conformational rigidity crystal packing effects as well as the solvent effects presumably slightly influencing the luminophores in the zinc and cadmium complexes. A greater red-shifted emission in the range 510−625 nm with Stokes shifts of about 110−225 nm is observed in the solid state in comparison to solution. This observation can be ascribed to efficient close packing[4g] (*vide infra* in the crystal structures) in **1**−**5** via $\pi\cdots\pi$ stacking/C−H$\cdots\pi$($ZnOSC_3$, chelate) interactions and to conformational rigidity as well as enhanced conjugation due to the Py(N) lone pair of electrons in the extended structures in **2**, **3**, and **5**. This clearly reveals the relationship between structure and luminescent properties in the complexes. Such packing interactions are further weakened in the solution phase.

Circular Dichroism Spectral Study. Complex **4** crystallized in chiral space group C2 of the monoclinic crystal system. Hence, its CD spectrum was recorded in DMSO solution to understand the chiral nature of the complex. The spectrum shows dichroic signals in the range 385−416 nm which correspond to the absorption maximum of the complex at 410 nm (inset) as depicted in Figure 2. The chirality of **4** probably originates from the twisted arrangement of the chelate ring (O_2S_2) of the β-oxodithioester ligand **L1** about the metal center (crystal structure discussion, *vide infra*).[18,28]

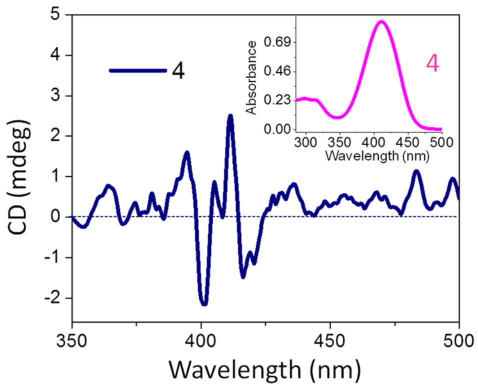

Figure 2. CD spectrum of complex **4** in DMSO.

Diffuse Reflectance Spectral Studies. The optical band gaps for complexes **1**−**5** were estimated by solid-state diffuse reflectance spectra (DRS) recorded against $BaSO_4$ as a reference at ambient temperature (Figure 3a). The reflectance spectra revealed that the complexes reflect wavelengths up to ca. 700 nm. This suggests that the corresponding energies are being used by the complexes for excitation of electrons from valence to conduction bands. The band gaps were calculated by using Planck's equation $E_{\text{band gap}} = hc/\lambda$, where h is Planck's constant ($4.135667516 \times 10^{-15}$ eV s), c is the velocity of light (2.998×10^8 m/s), and λ is the wavelength (nm). The suitable wavelength for band gap determination was determined by the first differential of diffuse reflectance spectra (Figure 3b).[17,29] Band gaps of 2.58, 2.50, 2.49, 2.62, and 2.57 eV have been observed in complexes **1**−**5**, respectively, which are in agreement with values derived from Kubelka−Munk functions[30] using the software package available with the Shimadzu UV-3101PC spectrometer (Figure 3b). Band gaps in the range 2.49−2.62 eV suggest a semiconductor behavior of the complexes.[17,29b,31]

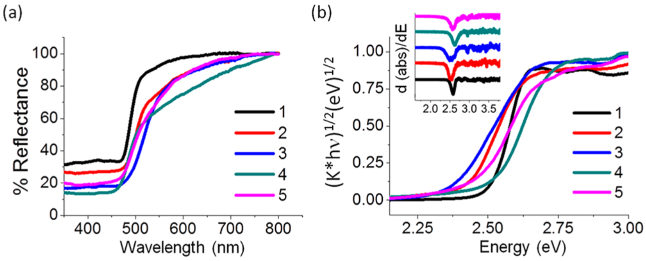

Figure 3. (a) Diffuse reflectance plots for solids **1**−**5** at room temperature using $BaSO_4$ as a reference. (b) Kubelka−Munk function vs energy plot for complexes **1**−**5**. The inset shows differentials of the solid-state absorbance of complexes with respect to radiation energy inflection points which give the band gap values.

Crystal Structures. Single crystals of **1**−**5** were grown from the saturated DMF solution of compounds within 2−3 weeks. Crystallographic data of all crystals and their structure refinement details are present in Table 1 while selected bond distances and angles are listed in Tables S1−S5 (Supporting Information). The **2**−**5** are the first examples of zinc(II) and cadmium(II) complexes with the functionalized β-oxodithioester ligands (L1−L3) displaying unique coordination polymeric structures.

The molecular structures of Zn and Cd complexes **1**−**5** are presented in Figures 4, 5a, 6a, 7a, and 8a, respectively. Except for complex **1**, which is monomeric, complexes **2**−**5** display polymeric structures. The mononuclear zinc complex **1** crystallizes in the monoclinic system with *C*2/*c* space group. The coordination geometry about the metal center, which occupies a 2-fold axis, is distorted tetrahedral, having O_2S_2 coordination from the two chelating β-oxodithioester ligands (**L1**) as presented in Figure 4. In **1**, the unique Zn−O and Zn−S distances are 1.967(3) and 2.285(1) Å respectively, which are comparable to the reported values,[4a,18] and the angles O(11)−Zn−S(15), O(11^1)−Zn−S(15), O11−Zn−O11^1, and S15−Zn−S15^1 are 101.67(8), 112.74(8), 105.28(16), and 121.94(6)°, respectively.

In **2**, the zinc atom lies on a crystallographic center of symmetry and is bonded by two β-oxodithioester ligands (L2) via (O^S) donor atoms in a chelating manner forming an O_2S_2 equatorial plane. The 3-pyridyl(N) groups on the adjacent molecules are interestingly weakly bonded to the metal atoms in axial positions, establishing an octahedral geometry with a $O_2S_2N_2$ core, overall forming a 12-membered metallacyclic

Table 1. Crystallographic Parameters for Complexes 1−5

complex	1	2	3	4	5
empirical formula	$C_{16}H_{14}O_2S_6Zn$	$C_{18}H_{16}N_2O_2S_4Zn$	$C_{18}H_{16}N_2O_2S_4Zn$	$C_{16}H_{14}O_2S_6Cd$	$C_{18}H_{16}N_2O_2S_4Cd$
formula wt	496.00	485.94	485.94	543.03	532.97
cryst syst	monoclinic	monoclinic	monoclinic	monoclinic	orthorhombic
space group	*C*2/*c*	*C*2/*c*	$P2_1/n$	*C*2	*Pbca*
a (Å)	23.755(4)	14.2134(18)	12.9400(3)	27.488(3)	15.3848(9)
b (Å)	4.9919(7)	9.7475(12)	12.1915(3)	3.9372(3)	14.4075(8)
c (Å)	16.989(3)	14.0086(12)	14.2632(3)	8.8421(6)	17.5204(11)
β (deg)	108.043(19)	96.831(10)	115.6240(10)	96.141(7)	90
V (Å^3)	1915.5(6)	1927.0(4)	2028.84(8)	951.45(13)	3883.5(4)
Z	4	4	4	2	8
ρ_{calc} (g cm^{-3})	1.720	1.675	1.591	1.895	1.823
T (K)	150(2)	150(2)	100(2)	150(2)	100(2)
μ(Mo Kα) (mm^{-1})	1.944	1.725	1.638	1.814	1.572
F(000)	1008	992	992	540	2128
no. of rflns collected	6182	4299	31931	2636	14884
no. of indep rflns	2737	2124	5045	1430	3434
no. of rflns with $I > 2\sigma(I)$	1957	1284	4603	1263	2272
final indices ($I > 2\sigma(I)$): R1,[a] wR2[b]	0.0615, 0.1356	0.0761, 0.1950	0.0223, 0.0699	0.0527, 0.1393	0.0448, 0.1168
R1,[a] wR2[b] (all data)	0.0898, 0.1535	0.1244, 0.2615	0.0261, 0.0735	0.0597, 0.1471	0.0858, 0.1416
GOF[c]	0.977	1.089	0.958	1.080	0.860
residual electron density (e Å^{-3})	1.569, −1.059	1.058, −0.706	0.395, −0.282	1.124, −1.275	1.353, −0.844
CCDC no.	1983320	1983319	1998352	1983318	1983321
Flack param				0.26(10)	

[a] $R1 = \sum||F_o| - |F_c||/\sum|F_o|$. [b] $wR2 = \{[\sum w(F_o^2 - F_c^2)/\sum w(F_o^2)^2]\}^{1/2}$. [c] $GOF = S = \{\sum[w(F_o^2 - F_c^2)^2]/(n - p)\}^{1/2}$, where n is the number of reflections and p is the number of refined parameters.

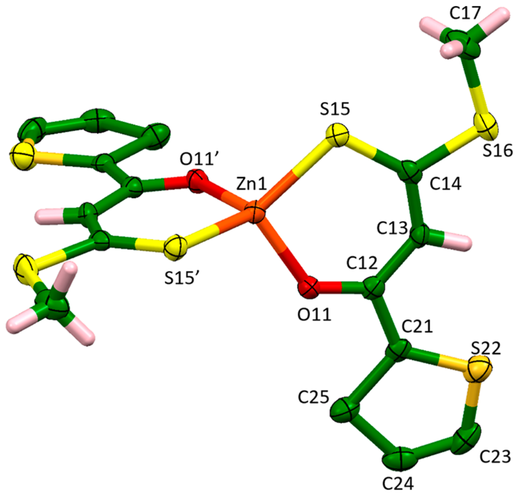

Figure 4. Molecular structure of **1** with ellipsoids at 50% probability showing the atom-numbering scheme. Hydrogen atoms of the thienyl ring are omitted for clarity.

ring leading to a linear 1D coordination polymeric structure (Figure 5b). The Zn−O, Zn−S, and Zn−N distances of 2.043(4), 2.363(2), and 2.455(6) Å, respectively, and the O(11)−Zn−S(15) angle of 93.79(12)° are well within the expected ranges.[4a,5,18] The energy of the interaction involving the formation of the two Zn−N axial bonds was calculated by taking three adjacent molecules into consideration. The single-point energy calculation evaluated from E(trimer) − 3E(monomer) is found to be −12.55 kcal mol^{-1}, thus indicating a significant interaction. For this purpose a trimeric model having three molecular units connected via Zn−N contacts was used, as depicted in Figure 5b. The coordinates were taken from the crystal structure.

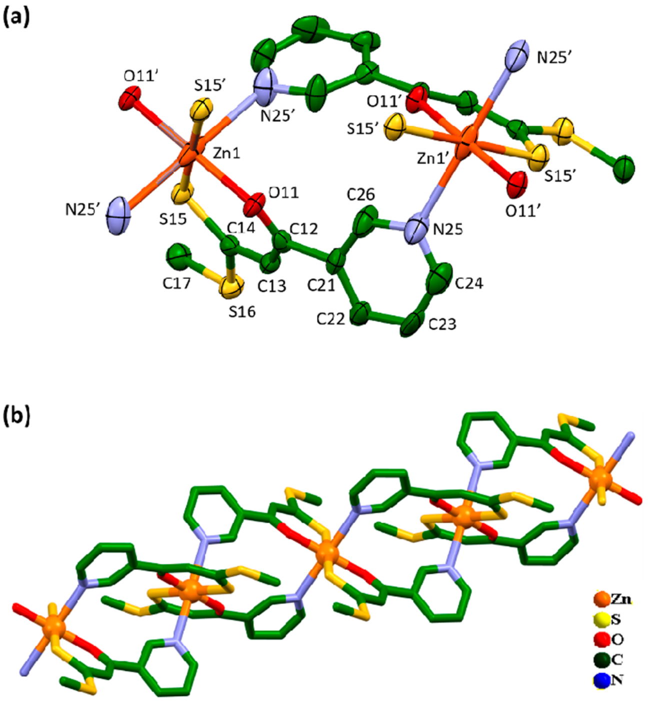

Figure 5. (a) Dimeric unit of **2** drawn with 50% probability for thermal ellipsoids. (b) 1D coordination polymeric chain running down the c axis in **2**, formed through intermolecular axial Zn−N bonds. Hydrogen atoms are omitted for clarity.

By comparison in **3**, the Zn atom occupies a general position and is chelated by two unique β-oxodithioester ligands (L3) via O^S-donor atoms in a bidentate manner. The two S atoms (S15, S35) together with N24 of the pyridine ring form a basal trigonal equatorial plane, NS_2. This equatorial plane along with the two apicophilic O11 and O31 atoms in the axial positions establish a trigonal-bipyramidal geometry about the Zn atoms, leading to a wavelike 1D coordination polymeric structure (Figure 6b). The Zn−S and Zn−N distances in the equatorial plane range from 2.3381(4) to 2.3476(4) and 2.0726(12) Å, respectively,[4a,5,18] and Zn−O distances at the axial positions are 2.0361(10) and 2.1013(10) Å. The τ value is 0.86, confirming the distorted-TBP geometry.

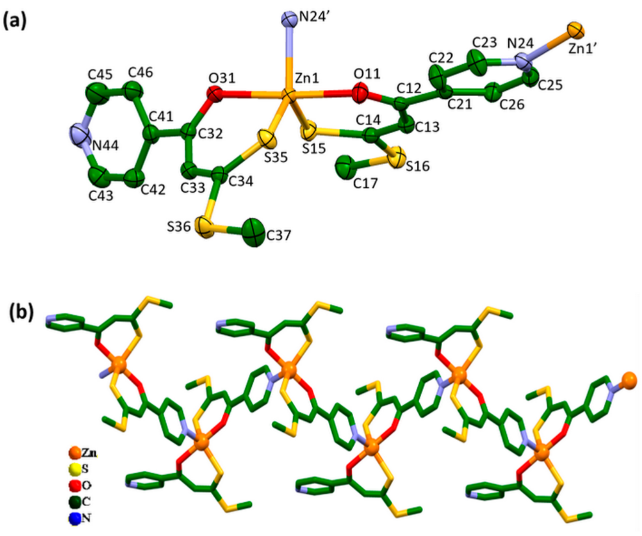

Figure 6. (a) Coordination environment of compound **3** showing the atom-numbering scheme depicted with 50% probability for thermal ellipsoids. H atoms are omitted for clarity. (b) Bridging coordination of **L3** via Zn−N bonds resulting in a wavelike 1D coordination polymeric chain running along the screw axis in the b direction. Hydrogen atoms are omitted for clarity.

The importance of the intermolecular bond to nitrogen is emphasized by a single-point calculation showing that the energy of interaction of two adjacent molecules with symmetry elements x, y, z and 3/2 − x, 1/2 + y, 3/2 − z, part of Figure 6b, given by E(dimer) − 2E(monomer) is −22.88 kcal mol^{-1}.

Unlike the tetrahedral zinc complex **1**, the Cd complex **4** crystallizes in the monoclinic system with chiral space group C2 with the metal situated on a 2-fold axis. The two β-oxodithioester ligands (**L1**) are bonded in a μ_2,κ^3-tridentate (O^S^S) coordination mode in contrast to the κ^2-bidentate (O^S) coordination mode observed in complex **1**. The Cd center is chelated by O11^S15-donor atoms and simultaneously is involved in bridging with another Cd atom through the S15 atom, establishing a distorted-octahedral coordination geometry. The bridging atoms facilitate the fusion of homochiral units to yield a 1D homochiral coordination polymeric structure (Figure 7b). The thienyl rings are severely disordered with four different arrangements in which there are two different orientations of the five-membered ring and then two different positions of the sulfur atom in each. Only the major component of this disorder is shown in Figure 7. The

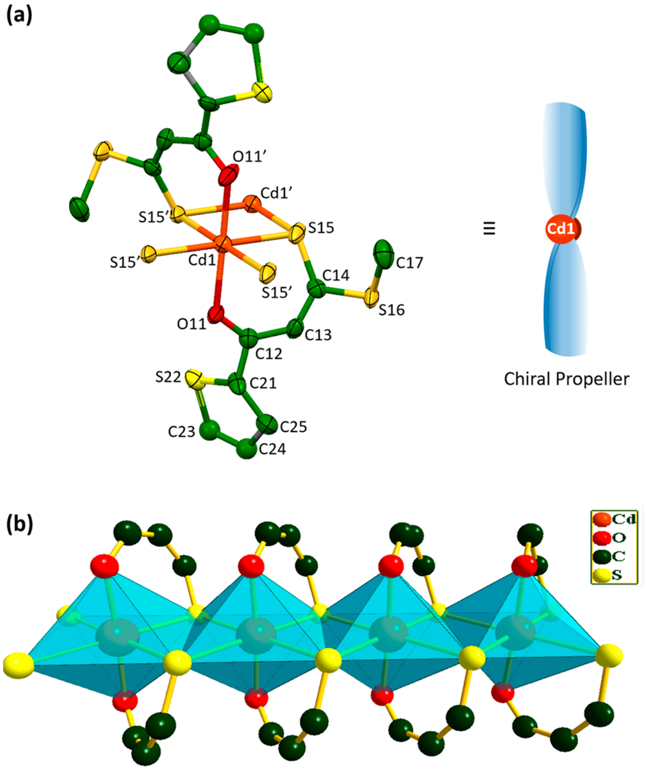

Figure 7. (a) Coordination environment of compound **4** showing the atom-numbering scheme depicted with 50% probability for thermal ellipsoids. The cadmium atom occupies a 2-fold axis. Only the major component of the disordered thienyl ring is shown. Hydrogen atoms are omitted for clarity. (b) Edge sharing of octahedral chiral propeller motifs along the *b* axis resulting in a 1D homochiral coordination polymeric chain. H atoms, −SMe groups, and thienyl substituents are omitted for clarity.

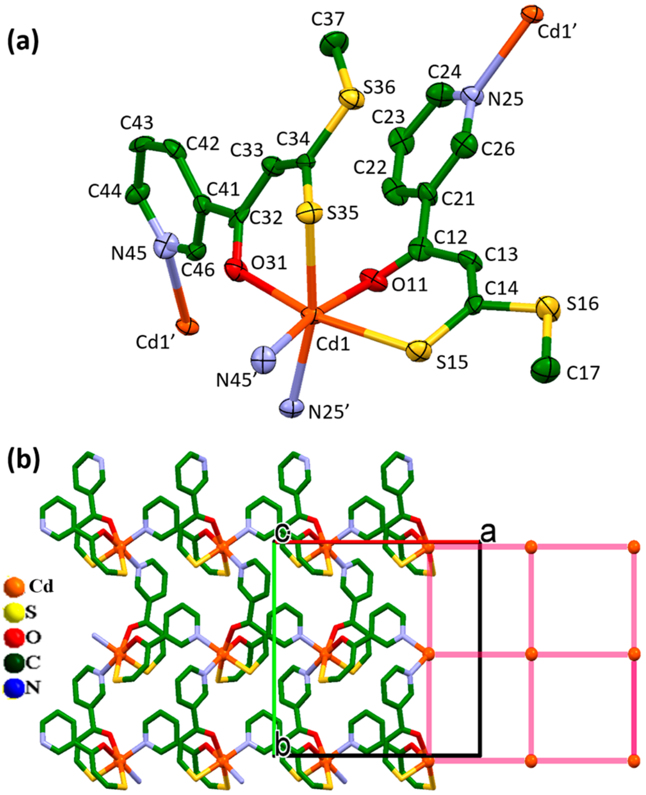

Figure 8. (a) Coordination environment of compound **5** showing the atom-numbering scheme depicted with 50% probability for thermal ellipsoids. Hydrogen atoms are omitted for clarity. (b) Packing diagram (down the *c* axis) depicting a 2D square lattice network in compound **5** stacked in an AAA pattern with its underlying *sql* topology presented on the right-hand side. Hydrogen atoms and −SMe groups are omitted for clarity.

preferential involvement of distinctly soft S atoms in bridging the neighboring Cd centers is in accordance with the HSAB principle. It is worth noting that, because of the orientation/constraint imposed by the six-membered chelate ring about the metal center, the chelating Cd−S distance at 2.719(6) Å is slightly longer than the bridging Cd−S distance at 2.691(6) Å. The Cd−O distance is 2.246(6) Å.[32] The geometry around the metal is a slightly distorted octahedron with the four sulfur atoms in an equatorial plane and the two oxygen atoms in axial positions, resulting in a propeller-shaped chiral motif (Figure 7a). The *cis* angles are in the range 86.0(2)−93.4(1)° and *trans* angles in the range 176.6(14)−179.4(2)°.

In complex **5**, the two unique β-oxodithioester ligands **L2** chelate to Cd atom through O^S donor atoms to form a Cd(L2)$_2$ unit (Figure 8a). The O^S donor atoms occupy four of the six coordination sites around the distorted-octahedral metal centers[32] with Cd−O distances of 2.303(5) and 2.313(5) Å and Cd−S distances of 2.641(2) and 2.570(2) Å. The remaining two mutually *cis* coordination sites are occupied by two 3-pyridyl(N) atoms from the two neighboring Cd(**L2**)$_2$ units with Cd−N distances of 2.342(5) and 2.422(5) Å, thus resulting in the formation of a 2D coordination polymeric square lattice with *sql* topology (Figure 8b). This polymeric structure also involves the formation of a 24-membered metallacyclic ring (Figure S9 in the Supporting Information).

It is interesting to note that complexes **1**−**5** form multidimensional structures which are stabilized by various weak noncovalent interactions such as C−H···π(ZnOSC$_3$, chelate), π···π, C−H···π, C−H···N and H···H interactions (Figures S2−S8 in the Supporting Information).

A noteworthy feature of the crystal packing of complexes **1** and **3** is the existence of supramolecular structures sustained by C−H···π (ZnOSC$_3$, chelate) interactions (Figures S2 and S5 in the Supporting Information), leading to a 1D supramolecular architecture via molecular aggregation. Recently, Tiekink and Zukerman-Schpector[33] evaluated the structural characteristics of C−H···π(chelate) interactions between C−H bonds and the centroid CG of four-membered MS$_2$C chelate rings in metal bis(1,1-dithiolates). For homoleptic bis-dithio complexes the values of $\alpha < 20$, β ranging from 110 to 180°, and d between 2.4 and 3.6 Å were crucial to assess the interactions where α is the angle between the perpendicular to the ring and the CG···H vector, β the CG···H−C angle, and d the CG···H distance.

In contrast in the present structures, there is a six-membered MSOC$_3$ ring and this ring is often found to be folded. In the structure of complex **1**, the rms deviation of the six atoms is 0.036 Å, whereas in complex **2** such rms deviations are 0.033 and 0.018 Å. However, in complex **3**, the atoms in the two rings have rms deviations of 0.018 and 0.234 Å, indicating that one ring is approximately planar while the other is folded. In complexes **4** and **5** the rings are folded, with the rms deviation in **4** being 0.208 Å and in **5** the two rings having rms deviations of 0.220 and 0.305 Å respectively. There is some correlation between the presence of H atom interactions with the planarity of the rings and presumably their aromaticity. In the structures of **1** and **3**, it is apparent that the hydrogen atoms of −SMe,

−SMe and pyridyl substituents occupy suitable axial positions for these types of interactions. Indeed in **1**, there are two such hydrogen atoms from the methyl group on the same side of the chelate ring from molecules with symmetry elements x, $1 + y$, z and $-x$, $-y$, $-z$ with the following respective values: α, 14 and 3; β, 157 and 131; d, 3.56 and 3.58 Å. These distances are relatively long in comparison to those found in the MS_2C rings referred to above, and we therefore calculated the energy of interaction between the two molecules involved in the interactions using the formula $E(\text{dimer}) - 2E(\text{monomer})$. Using molecules with symmetry elements x, y, z and x, $1 + y$, z the energy of interaction was -3.56 kcal mol^{-1} and with molecules x, y, z and $-x$, $-y$, $-z$ the energy was -3.85 kcal mol^{-1}. However, a shorter contact is found in complex **3** to the near-planar ring with an intramolecular contact in which α, β, and d are 14°, 120°, and 2.69 Å, respectively.

Catalytic Studies. Complexes **1**−**5** have been investigated as catalysts for the Knoevenagel condensation and one-pot multicomponent reactions. To the best of our knowledge, this is the first report in which Zn(II) and Cd(II) with β-oxodithioester ligands have been synthesized and used as catalysts in C−C bond formation reactions. The presence of the exposed Lewis acidic sites (Zn^{2+}/Cd^{2+} centers) and basic sites (pyridyl-N) in the complexes encouraged us to explore their abilities in the organic transformation reactions.

Knoevenagel Condensation Reaction. The Knoevenagel condensation is a well-known synthetic methodology to construct a C−C bond from an aldehyde and a compound containing an activated methylene group. This reaction is highly effective in the organic synthesis of biologically important compounds[34] and also fine chemicals.[35] Although Knoevenagel condensation reactions are catalyzed by amine bases in excess quantity under homogeneous conditions,[36] several Lewis acid catalysts have also been successfully utilized under heterogeneous conditions and these are always preferred due to their stability, potential recyclability, and ease of product separation.[8,10]

The catalytic activities of complexes **1**−**5** were evaluated in the Knoevenagel condensation reaction. The screening of complexes as catalysts was assessed by a model reaction involving the reaction of benzaldehyde with malononitrile in the presence of 5 mol % of the complex as a catalyst in methanol at 60 °C, which resulted in the formation of benzylidene malononitrile as the principal product (Table 2). Although the polarity of solvents has a great effect on the catalytic reaction,[10c,d] we chose methanol as solvent in the catalysis due to the insolubility of complexes in it and, hence, reactions could be performed heterogeneously. However, a high catalytic activity of complex **3** was also observed when DMSO was used as the solvent in the reaction. We observed 100% consumption of benzaldehyde in less than 20 min. Since complex **3** is soluble in DMSO, i.e. homogeneous catalysis, this resulted in difficulties regarding separation of the catalyst and lack of catalyst recyclability. Therefore, homogeneous catalysis is practically undesirable in this case.

The Knoevenagel reaction does occur in the absence of a catalyst, but it is very slow and only a 30% yield was obtained in 4 h (Table 2, entry 1). Similar results have also been obtained when zinc complex **2** and cadmium complexes **4** and **5** were used in the reaction (Table 2, entries 3 and 5−7). On the other hand, complexes **1** and **3** afforded excellent yields and we observed >95% isolated yields in 2 h (for complex **1**; Table 2, entry 2) and 1 h (for complex **3**; Table 2, entry 4).

Table 2. Catalyst Screening for the Knoevenagel Condensation of Benzaldehyde with Malononitrile[a]

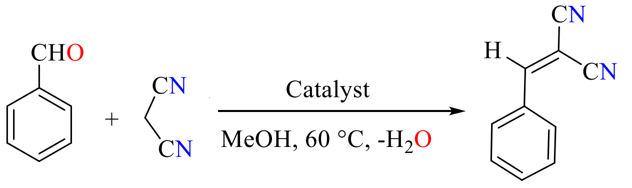

entry	catalyst (5 mol %)	time (h)	yield[b] (%)
1		4	30
2[c]	1	2	96
3	2	4	30
4[c]	3	1	98
5	4	4	30
6	5	4	30

[a] Reaction conditions: benzaldehyde (1.0 mmol), malononitrile (1.0 mmol), MeOH (5 mL) in an air atmosphere. [b] Isolated yield. [c] 100% consumption of benzaldehyde.

The metal centers in complexes **2**, **4**, and **5** exhibited octahedral coordination geometries, and therefore, the possibility of activation of benzaldehyde by metal complexes was insignificant. Interestingly, the geometries around metal centers in complexes **1** and **3** are distorted tetrahedral and TBP, respectively, which may allow the benzaldehyde to interact with Zn^{2+} ions and hence result in high activities. Furthermore, it is interesting to note that pyridyl-N at one of the ligands coordinated to the Zn^{2+} metal ion in complex **3** is not engaged in the bonding and thus might participate in one of the steps in the catalytic cycle, namely proton abstraction from malononitrile and, therefore, easy generation of nucleophile. The catalytic studies have revealed that complex **3** behaves as a bifunctional catalyst and therefore an excellent yield was promoted synergistically by Lewis acidic and basic sites of the complex.

There have been a few reports[10] describing bifunctional role (acidic and basic) of MOFs as heterogeneous catalysts in the Knoevenagel condensation reactions (Table S7). MOFs can act as Lewis acids or bases in the catalytic reactions depending on the nature of the ligands, the metal ions, and coordination environment around the metal centers. Zhou and co-workers[10a] studied a one-pot tandem deacetalization−Knoevenagel condensation reaction for the synthesis of benzylidene malononitrile using PCN-124 MOF as a heterogeneous catalyst. The weakly Lewis acidic open Cu^{2+} centers and Lewis basic pyridine as well as amide functionalities of PCN-124 made this MOF useful for one-pot tandem reactions. Similarly, a tandem Meinwald rearrangement−Knoevenagel condensation reaction catalyzed by the bifunctional catalyst NH_2-MIL-101(Al) with remarkable substrate selectivity was reported by Kim and co-workers.[10b] Yang et al. also reported an amine-functionalized Zr based MOF; UiO-66-NH_2 possessing acidic (Zr) and basic ($-NH_2$) sites showed 98% conversion of aldehyde to benzylidene malononitrile in the Knoevenagel condensation reaction.[10c] In recent years, some Zn(II) and Cd(II) MOFs have also been utilized as bifunctional heterogeneous catalysts in the Knoevenagel reactions. Suresh and co-workers reported Zn(II) and Cd(II) MOFs as potential bifunctional catalysts under ambient conditions with excellent yield.[10d] A cationic Zn(II)−organic framework with Lewis acidic and basic bifunctional sites has also exhibited high activity and substrate selectivity under solvent-free reaction conditions.[10e] A very high catalytic activity was achieved in the Knoevenagel condensation reaction using a Zn(II)-based metal−organic framework, Zn-Bp-BTC MOF, as an effective bifunctional heterogeneous catalyst.[10f]

To explore the catalytic performance of complex **3**, the reactions of several benzaldehyde derivatives, 1-naphthaldehyde and heteroaromatic aldehydes, with malononitrile have been studied (Table 3). The nature of the substituent on the benzaldehyde ring has a considerable effect on the yield of the product. Electron-withdrawing substituents, e.g. fluoro, chloro, nitro, cyano, and hydroxy, at the para position of benzaldehyde and the 3,4,5-trimethoxy substituent are more effective and gave excellent yields (Table 3, entries 2−7). In contrast, electron-donating substituents (methyl and methoxy) at the para position of benzaldehyde made the reaction slow and resulted in a lower product yield (Table 3, entries 8 and 9). A fused aromatic system (1-naphthaldehyde) and heteroaromatic aldehydes (2-thienylcarboxaldehyde and 4-pyridinecarboxaldehyde) provided slow reactions and also lower yields (Table 3, entries 10−12).

Multicomponent Reaction: Synthesis of 2-Amino-4H-chromene Derivatives. We have also explored the usefulness of complex **3** as a catalyst for multicomponent condensation reactions of aromatic aldehyde, malononitrile, and active methylene cyclic 1,3-diketone derivatives, resulting in the formation of 2-amino-4*H*-chromene derivatives, which are an important class of heterocyclic compounds possessing biological and pharmaceutical properties.[37] The catalytic results are summarized in Table 4. The one-pot reaction of benzaldehyde, malononitrile, and cyclohexane-1,3-dione in ethanol at 80 °C does not occur in the absence of catalyst **3** (Table 4, entry 1). However, the addition of the catalyst facilitated the reaction and afforded the product in 97% isolated yield (Table 4, entry 2). The reaction was also studied using different types of aromatic aldehydes, and high yields of the desired products were obtained with 1-naphthaldehyde, 2-thienylcarboxaldehyde, and 4-pyridinecarboxaldehyde (Table 4, entries 3−5). It is interesting to note that when cyclohexane-1,3-dione was replaced with either 5,5-dimethylcyclohexane-1,3-dione (entries 6−9) or 5-phenylcyclohexane-1,3-dione (entries 10−13) excellent yields of the corresponding products were obtained. Kathiresan and co-workers have also achieved a very high yield of 2-amino-4*H*-chromene derivatives (>90%) using Zn-Bp-BTC MOF as a heterogeneous catalyst, but they ran the reaction for a longer time (5 h).[10f] It can be seen that the Zn(II) *β*-oxodithioester complex showed promising catalytic activity for the one-pot multicomponent synthesis of 2-amino-4*H*-chromene derivatives.

Recyclability of the Catalyst. The catalyst recyclability is an essential requirement in the heterogeneous catalysis. Therefore, we also evaluated the recyclability of catalyst **3** in the Knoevenagel condensation reaction of benzaldehyde and malononitrile under optimized reaction conditions. At the end of the reaction, catalyst **3** was simply collected by filtration, washed three times using methanol, dried, and reused in a consecutive reaction. Notably, complete consumption of benzaldehyde with over 96% isolated yield of product was observed for five recycles (Figure S10a in the Supporting Information). Also, characterization of the recovered catalyst by PXRD showed the retention of catalyst integrity (Figure S10b in the Supporting Information).

Table 3. Knoevenagel Condensation Reactions of Aromatic Aldehydes with Malononitrile Using Catalyst 3[b]

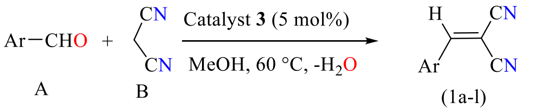

Entry	Ar	Product	Yield[a] %
1	C_6H_5	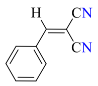 1a	98
2	$4\text{-}FC_6H_4$	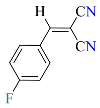 1b	98
3	$4\text{-}ClC_6H_4$	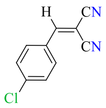 1c	98
4	$4\text{-}NO_2C_6H_4$	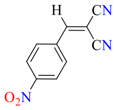 1d	97
5	$4\text{-}CNC_6H_4$	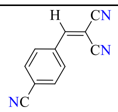 1e	96
6	$3,4,5\text{-}(MeO)_3C_6H_2$	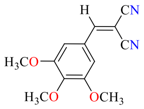 1f	98
7	$4\text{-}OHC_6H_4$	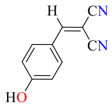 1g	96
8	$4\text{-}MeC_6H_4$	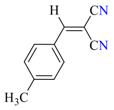 1h	91
9	$4\text{-}OMeC_6H_4$	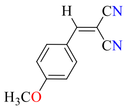 1i	89
10	1-Naphthalenyl	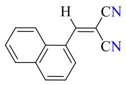 1j	94
11	2-Thienyl	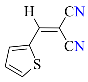 1k	92
12	4-Pyridyl	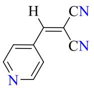 1l	89

[a] Isolated yield. [b] Reaction conditions: aldehyde (1.0 mmol), malononitrile (1.0 mmol), MeOH (5 mL), temperature (60 °C), time (1 h) in an air atmosphere.

Table 4. One-Pot Multicomponent Reactions for Synthesis of 2-Amino-4*H*-chromene Derivatives[c]

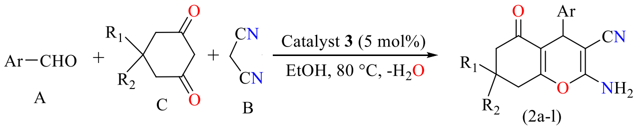

$R_1, R_2 = H$
$R_1 = H$, and $R_2 = CH_3$, Phenyl

Entry	Ar	Diketone	Product	Yield^{a} (%)
1	Phenyl	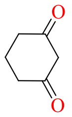	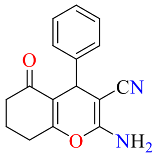 2a	–^{b}
2	Phenyl	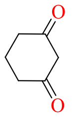	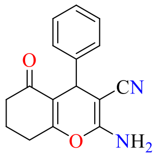 2a	97
3	1-Naphthalenyl	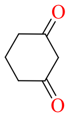	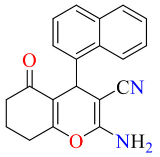 2b	94
4	2-Thienyl	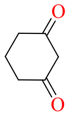	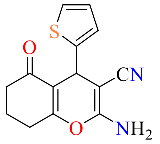 2c	92
5	4-Pyridyl	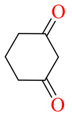	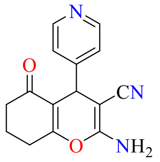 2d	87
6	Phenyl	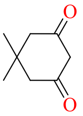	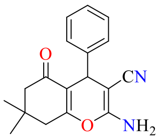 2e	98
7	1-Naphthalenyl	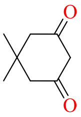	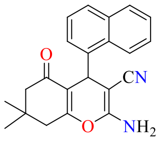 2f	98
8	2-Thienyl	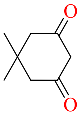	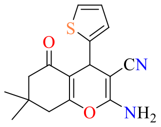 2g	93
9	4-Pyridyl	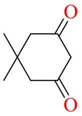	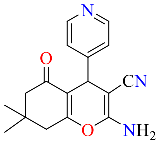 2h	89
10	Phenyl	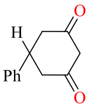	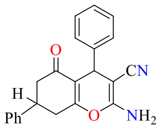 2i	97
11	1-Naphthalenyl	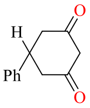	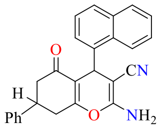 2j	94
12	2-Thienyl	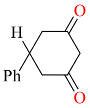	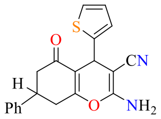 2k	92
13	4-Pyridyl	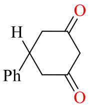	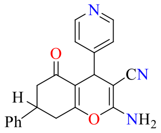 2l	86

[a]Isolated yield. [b]Reaction without catalyst. [c]Reaction conditions: aldehyde (1.0 mmol), malononitrile (1.0 mmol), 1,3-diketone (1.0 mmol), EtOH (5 mL), temperature (80 °C), time (1.5 h) in an air atmosphere.

Plausible Mechanism for the Knoevenagel and Multicomponent Reactions. The reaction mechanisms for the Knoevenagel condensation and one-pot multicomponent reactions have been well documented in the literature (Scheme S1 in the Supporting Information).[10d,f,38] The Knoevenagel condensation reaction of benzaldehyde with malononitrile proceeds first via the activation of benzaldehyde by the catalyst **3**, which increases the electrophilicity of the carbonyl carbon (**I**). The activated aldehyde is now attacked by the malononitrile nucleophile, $(CN)_2CH^-$ (**II**), generated by proton abstraction, which leads to C—C bond formation (**III**). In the next step, the intermediate is dissociated from the catalyst surface and undergoes dehydration to give the final benzylidene malononitrile as the Knoevenagel product-I and the catalyst is regenerated.[10d,f]

The multicomponent reaction involves the attack of enolate generated from 1,3-cyclohexanedione (**VI**) on the *in situ* generated Knoevenagel condensation product-I, resulting in a second C—C bond formation via a Michael addition reaction (**VII**).[38] This is followed by tautomerization and intramolecular cyclization (C—O bond formation) to afforded the

2-amino-4*H*-chromene derivative as multicomponent reaction product-II.

■ CONCLUSIONS

Novel heteroleptic Zn(II) and Cd(II) complexes **1**−**5** with functionalized *β*-oxodithioester ligands have been synthesized and fully characterized. The solid-state molecular structures revealed that complex **1** is a tetrahedral monomer, whereas complexes **2**−**4** are spectacular 1D coordination polymers and **5** is a 2D coordination polymer. In these complexes, *β*-oxodithioester ligands act as suitable linkers for the construction of metal−organic frameworks utilizing O^S-chelates and bridges along with pyridyl(N). Complex **3** displayed efficient heterogeneous catalytic activity in the Knoevenagel condensation and one-pot multicomponent reactions. The higher catalytic performance of trigonal bipyramidal complex **3** is attributed to its Lewis acidic character due to the coordinative unsaturation around Zn^{2+} and the presence of a free 4-pyridyl(N) substituent, which serves as a Lewis base. Hence, complex **3** behaves as a bifunctional catalyst and could be recycled five times without an obvious decrease in activity. The zinc complexes strongly luminesce in the solid state whereas the cadmium complexes showed luminescent characteristics in solution, which may be ascribed to the changes in luminophores of the complexes in the different media, though in both cases the emission emanates from the metal-perturbed intraligand charge transfer transitions (ILCTs). In addition, the band gap values (2.49−2.62 eV) evaluated from DRS studies indicated the semiconductor characteristics of the complexes. The electronic and steric characteristics of the substituents on the *β*-oxodithioester backbone have a significant effect on the structures and properties of the complexes. This study demonstrates that the zinc(II) and cadmium(II) complexes of functionalized *β*-oxodithioesters may be useful for the design of new compounds with promising material properties.

■ ASSOCIATED CONTENT

Supporting Information

The Supporting Information is available free of charge at https://pubs.acs.org/doi/10.1021/acs.inorgchem.0c01195.

^{1}H and $^{13}C\{^{1}H\}$ NMR spectra, FT-IR spectra, UV−vis spectra, PXRD, details of selected bond lengths and angles for complexes **1**−**5**, supporting crystallographic figures, and characterization data for the Knoevenagel condensation and multicomponent products (PDF)

Accession Codes

CCDC 1983318−1983321 and 1998352 contain the supplementary crystallographic data for this paper. These data can be obtained free of charge via www.ccdc.cam.ac.uk/data_request/cif, or by emailing data_request@ccdc.cam.ac.uk, or by contacting The Cambridge Crystallographic Data Centre, 12 Union Road, Cambridge CB2 1EZ, UK; fax: +44 1223 336033.

■ AUTHOR INFORMATION

Corresponding Author

Nanhai Singh − *Department of Chemistry, Institute of Science, Banaras Hindu University, Varanasi 221005, India;* orcid.org/0000-0003-1578-5456; Email: nsinghbhu@gmail.com, nsingh@bhu.ac.in

Authors

Chote Lal Yadav − *Department of Chemistry, Institute of Science, Banaras Hindu University, Varanasi 221005, India;* orcid.org/0000-0003-1535-5018

Anamika − *Department of Chemistry, Institute of Science, Banaras Hindu University, Varanasi 221005, India;* orcid.org/0000-0001-8070-710X

Gunjan Rajput − *Department of Chemistry, RCU Government Post Graduate College, Uttarkashi 249193, India;* orcid.org/0000-0002-7714-8164

Kamlesh Kumar − *Department of Chemistry, Institute of Science, Banaras Hindu University, Varanasi 221005, India;* orcid.org/0000-0001-7374-5941

Michael G. B. Drew − *Department of Chemistry, University of Reading, Reading RG6 6AD, U.K.;* orcid.org/0000-0001-8687-3440

Complete contact information is available at: https://pubs.acs.org/10.1021/acs.inorgchem.0c01195

Author Contributions

The manuscript was written through contributions of all authors.

Notes

The authors declare no competing financial interest.

■ ACKNOWLEDGMENTS

We gratefully acknowledge financial support from the University Grants Commission (UGC), New Delhi, for the award of a BSR Faculty Fellow (ref, no. F. 18-1/2011(BSR)) Dec 2016 to N.S., a UGC-SRF fellowship to C.L.Y., and a UGC-BSR Research Start-Up-Grant (No. F. 30-431/2018 (BSR)) to K.K.. G.R. acknowledges the Department of Science and Technology (DST), New Delhi, for a DST-INSPIRE Faculty fellowship (award ref. no. DST/INSPIRE/04/2016/000997). We are also thankful to the Department of Chemistry, Institute of Science, Banaras Hindu University, UGC CAS-II, for infrastructural facilities and the University of Reading, EPSRC (UK), for funds for the diffractometers used in the data collections.

■ REFERENCES

(1) O'keeffe, M.; Yaghi, O. M. Deconstructing the Crystal Structures of Metal_Organic Frameworks and Related Materials into Their Underlying Nets. *Chem. Rev.* **2012**, *112*, 675−702.

(2) (a) Cook, T. R.; Zheng, Y. R.; Stang, P. J. Metal-Organic Frameworks and Self-Assembled Supramolecular Coordination Complexes: Comparing and Contrasting the Design, Synthesis, and Functionality of Metal-Organic Materials. *Chem. Rev.* **2013**, *113*, 734−777. (b) Cook, T. R.; Stang, P. J. Recent Developments in the Preparation and Chemistry of Metallacycles and Metallacages via Coordination. *Chem. Rev.* **2015**, *115*, 7001−7045.

(3) (a) Hogarth, G. Transition metal dithiocarbamates. *Prog. Inorg. Chem.* **2005**, *53*, 71−561. (b) Batten, S. R.; Neville, S. M.; Turner, D. R. *Coordination Polymers Design, Analysis and Application*, 1st ed.; RSC Publishing: Cambridge, U.K., 2009. (c) Anamika; Yadav, D. K.; Manar, K. K.; Yadav, C. L.; Kumar, K.; Ganesan, V.; Drew, M. G. B.; Singh, N. New heteroleptic [Ni(II) 1,1-dithiolate-phosphine] complexes: synthesis, characterization and electrocatalytic oxygen evolution studies. *Dalton Trans.* **2020**, *49*, 3592−3605.

(4) (a) Fu, R.; Xiang, S.; Hu, S.; Wang, L.; Li, Y.; Huang, X.; Wu, X. Assembled bright green fluorescence zinc coordination polymer. *Chem. Commun.* **2005**, 5292−5294. (b) Janiak, C. Engineering coordination polymers towards applications. *Dalton Trans.* **2003**, 2781−2804. (c) Dai, J. C.; Wu, X. T.; Fu, Z. Y.; Cui, C. P.; Hu, S. M.;

Du, W. X.; Wu, L. M.; Zhang, H. H.; Sun, R. Q. Synthesis, Structure, and Fluorescence of the Novel Cadmium(II)−Trimesate Coordination Polymers with Different Coordination Architectures. *Inorg. Chem.* **2002**, *41*, 1391−1396. (d) Kumar, V.; Singh, V.; Gupta, A. N.; Manar, K. K.; Drew, M. G. B.; Singh, N. Influence of ligand environments on the structures and luminescence properties of homoleptic cadmium(II) pyridyl functionalized dithiocarbamates. *CrystEngComm* **2014**, *16*, 6765−6774. (e) Singh, V.; Kumar, V.; Gupta, A. N.; Drew, M. G. B.; Singh, N. Effect of pyridyl substituents leading to the formation of green luminescent mercury(II) coordination polymers, zinc(II) dimers and a monomer. *New J. Chem.* **2014**, *38*, 3737−3748. (f) Kang, J.-G.; Shin, J.-S.; Cho, D.-H.; Jeong, Y.-K.; Park, C.; Soh, S. F.; Lai, C. S.; Tiekink, E. R. T. Steric Control over Supramolecular Polymer Formation in trans-1,2-Bis(4-pyridyl)ethylene Adducts of Zinc Xanthates: Implications for Luminescence. *Cryst. Growth Des.* **2010**, *10*, 1247−1256. (g) Kushvaha, S. K.; Arumugam, S.; Shankar, B.; Sarkar, R. S.; Ramkumar, V.; Mondal, K. C. Isolation and Characterization of Different Homometallic and Heterobimetallic Complexes of Nickel and Zinc Ions by Controlling Molar Ratios and Solvents. *Eur. J. Inorg. Chem.* **2019**, *2019*, 2871−2882. (h) Tang, Y.-Z.; Zhou, M.; Huang, J.; Tan, Y.-H.; Wu, J.-S.; Wen, H.-R. In Situ Synthesis and Ferroelectric, SHG Response, and Luminescent Properties of a Novel 3D Acentric Zinc Coordination Polymer. *Inorg. Chem.* **2013**, *52*, 1679−1681.

(5) (a) Smith, J. N.; Shirin, Z.; Carrano, C. J. Control of Thiolate Nucleophilicity and Specificity in Zinc Metalloproteins by Hydrogen Bonding: Lessons from Model Compound Studies. *J. Am. Chem. Soc.* **2003**, *125*, 868−869. (b) Ma, L.-F.; Li, C.-P.; Wang, L.-Y.; Du, M. Zn(II) and Cd(II) Coordination Polymers Assembled from a Versatile Tecton 5-Nitro-1,2,3-benzenetricarboxylic Acid and N, N0-Donor Ancillary Coligands. *Cryst. Growth Des.* **2010**, *10*, 2641−2649.

(6) (a) Zhu, L.; Liu, X.-Q.; Jiang, H.-L.; Sun, L.-B. Metal-Organic Frameworks for Heterogeneous Basic Catalysis. *Chem. Rev.* **2017**, *117*, 8129−8176. (b) Chughtai, A. H.; Ahmad, N.; Younus, H. A.; Laypkov, A.; Verpoort, F. Metal−organic frameworks: versatile heterogeneous catalysts for efficient catalytic organic transformations. *Chem. Soc. Rev.* **2015**, *44*, 6804−6849. (c) Markad, D.; Mandal, S. K. Design of a Primary-Amide-Functionalized Highly Efficient and Recyclable Hydrogen-Bond-Donating Heterogeneous Catalyst for the Friedel-Crafts Alkylation of Indoles with β-Nitrostyrenes. *ACS Catal.* **2019**, *9*, 3165−3173.

(7) (a) Dhakshinamoorthy, A.; Asiri, A. M.; Garcia, H. Metal−organic frameworks catalyzed C−C and C−heteroatom coupling reactions. *Chem. Soc. Rev.* **2015**, *44*, 1922−1947. (b) Olah, G. A.; Molnar, A. *Hydrocarbon Chemistry*; Wiley: New York, 1995. (c) Hu, M.-L.; Safarifard, V.; Doustkhah, E.; Rostamnia, S.; Morsali, A.; Nouruzi, N.; Beheshti, S.; Akhbari, K. Taking organic reactions over metal-organic frameworks as heterogeneous catalysis. *Microporous Mesoporous Mater.* **2018**, *256*, 111−127. (d) Pascanu, V.; González Miera, G.; Inge, A. K.; Martin-Matute, B. Metal-Organic Frameworks as Catalysts for Organic Synthesis: A Critical Perspective. *J. Am. Chem. Soc.* **2019**, *141*, 7223−7234. (e) Li, Y.; Zhang, X.; Lan, J.; Xu, P.; Sun, J. Porous Zn(Bmic)(AT) MOF with Abundant Amino Groups and Open Metal Sites for Efficient Capture and Transformation of CO_2. *Inorg. Chem.* **2019**, *58*, 13917−13926.

(8) (a) Tran, U. P. N.; Le, K. K. A.; Phan, N. T. S. Expanding Applications of Metal-Organic Frameworks: Zeolite Imidazolate Framework ZIF-8 as an Efficient Heterogeneous Catalyst for the Knoevenagel Reaction. *ACS Catal.* **2011**, *1*, 120−127. (b) Neogi, S.; Sharma, M. K.; Bharadwaj, P. K. Knoevenagel condensation and cyanosilylation reactions catalyzed by a MOF containing coordinatively unsaturated Zn(II) centers. *J. Mol. Catal. A: Chem.* **2009**, *299*, 1−4. (c) Pachisia, S.; Gupta, R. Two Hg(II)-Based Macrocycles Offering Hydrogen Bonding Cavities: Influence of Cavity Structure on Heterogeneous Catalysis. *Cryst. Growth Des.* **2019**, *19*, 6039−6047.

(9) (a) Kurono, N.; Ohkuma, T. Catalytic Asymmetric Cyanation Reactions. *ACS Catal.* **2016**, *6*, 989−1023. (b) Liang, G.-M.; Xiong, P.; Azam, K.; Ni, Q.-L.; Zeng, J.-Q.; Gui, L.-C.; Wang, X.-J. A Discrete Tetrahedral Indium Cage as an Efficient Heterogeneous Catalyst for the Fixation of CO_2 and the Strecker Reaction of Ketones. *Inorg. Chem.* **2020**, *59*, 1653−1659. (c) List, B.; Lerner, R. A.; Barbas, C. F. Proline-Catalyzed Direct Asymmetric Aldol Reactions. *J. Am. Chem. Soc.* **2000**, *122*, 2395−2396. (d) Zhou, Y.; Song, J.; Liang, S.; Hu, S.; Liu, H.; Jiang, T.; Han, B. Metal-organic frameworks as an acid catalyst for the synthesis of ethyl methyl carbonate via transesterification. *J. Mol. Catal. A: Chem.* **2009**, *308*, 68−75. (e) Jacobsen, E. N.; Zhang, W.; Muci, A. R.; Ecker, J. R.; Deng, L. Highly enantioselective epoxidation catalysts derived from 1,2-diaminocyclohexane. *J. Am. Chem. Soc.* **1991**, *113*, 7063−7064. (f) Opelt, S.; Turk, S.; Dietzsch, E.; Henschel, A.; Kaskel, S.; Klemm, E. Preparation of palladium supported on MOF-5 and its use as hydrogenation catalyst. *Catal. Commun.* **2008**, *9*, 1286−1290. (g) Liu, H.; Liu, Y.; Li, Y.; Tang, Z.; Jiang, H. J. Metal-Organic Framework Supported Gold Nanoparticles as a Highly Active Heterogeneous Catalyst for Aerobic Oxidation of Alcohols. *J. Phys. Chem. C* **2010**, *114*, 13362−13369. (h) Phan, N. T. S.; Le, K. K. A.; Phan, T. D. MOF-5 as an efficient heterogeneous catalyst for Friedel−Crafts alkylation reactions. *Appl. Catal., A* **2010**, *382*, 246−253. (i) Marcelli, T.; van der Haas, R. N. S.; van Maarseveen, J. H.; Hiemstra, H. Asymmetric Organocatalytic Henry Reaction. *Angew. Chem., Int. Ed.* **2006**, *45*, 929−931. (j) Miyaura, N.; Suzuki, A. Palladium-Catalyzed Cross-Coupling Reactions of Organoboron Compounds. *Chem. Rev.* **1995**, *95*, 2457−2483. (k) Berner, O. M.; Tedeschi, L.; Enders, D. Asymmetric Michael Additions to Nitroalkenes. *Eur. J. Org. Chem.* **2002**, *2002*, 1877−1894.

(10) (a) Park, J.; Li, J.-R.; Chen, Y.-P.; Yu, J.; Yakovenko, A. A.; Wang, Z. U.; Sun, L.-B.; Balbuena, P. B.; Zhou, H.-C. A versatile metal−organic framework for carbon dioxide capture and cooperative catalysis. *Chem. Commun.* **2012**, *48*, 9995−9997. (b) Srirambalaji, R.; Hong, S.; Natarajan, R.; Yoon, M.; Hota, R.; Kim, Y.; Ko, Y. H.; Kim, K. Tandem catalysis with a bifunctional site-isolated Lewis acid−Brønsted base metal−organic framework, NH_2-MIL-101(Al). *Chem. Commun.* **2012**, *48*, 11650−11652. (c) Yang, Y.; Yao, H.-F.; Xi, F.-G.; Gao, E.-Q. Amino-functionalized Zr(IV) metal−organic framework asbifunctional acid−base catalyst for Knoevenagel condensation. *J. Mol. Catal. A: Chem.* **2014**, *390*, 198−205. (d) Parmar, B.; Patel, P.; Murali, V.; Rachuri, Y.; Kureshy, R. I.; Khan, N. H.; Suresh, E. Efficient Heterogeneous Catalysis by Dual Ligand Zn(II)/Cd(II) MOFs for Knoevenagel Condensation Reaction: Adaptable Synthetic Routes, Characterization, Crystal Structure and Luminescence Studies. *Inorg. Chem. Front.* **2018**, *5*, 2630−2640. (e) Yao, C.; Zhou, S.; Kang, X.; Zhao, Y.; Yan, R.; Zhang, Y.; Wen, L. A Cationic Zinc-Organic Framework with Lewis Acidic and Basic Bifunctional Sites as an Efficient Solvent-Free Catalyst: CO_2 Fixation and Knoevenagel Condensation Reaction. *Inorg. Chem.* **2018**, *57*, 11157−11164. (f) Madasamy, K.; Kumaraguru, S.; Sankar, V.; Mannathan, S.; Kathiresan, M. Zn based Metal Organic Framework as a Heterogeneous Catalyst for C−C Bond Formation Reactions. *New J. Chem.* **2019**, *43*, 3793−3800.

(11) (a) Liu, C.-Y.; Lih, J.-J. Synthesis, characterization and complexation properties of a polystyrene resin containing β-hydroxydithiocinnamic acid. *Fresenius' Z. Anal. Chem.* **1988**, *332*, 171−175. (b) Lih, J. J.; Yeh, K. Y.; Liu, C. Y. Chromatographic separation by a new chelating resin containing-hydroxydithiocinnamic acid. *Fresenius' J. Anal. Chem.* **1990**, *336*, 12−15.

(12) (a) Galan-Vidal, C. A.; Paez-Hernandez, M. E.; Cuellar-Cruz, M.; Perez- Lopez, B.; Lopez-Martinez, E.; Pliego-Canton, T. C.; Alvarez Toledano, C. Silver [I] PVC ion-selective membrane electrode based on 3, 3-dithio-1-[p-methyl] phenyl-2-propen-1 one as ionophore. *Sens. Chemom.* **2001**, 39−46. (b) Galan-Vidal, C. A.; Paez-Hernandez, M. E.; Cuellar-Cruz, M.; Perez- Lopez, B.; Portillo-Ortega, G.; Alvarez-Toledano, C. Use of 3, 3-dithio-1-(para-methyl) phenyl-2-propen-1-one for recovery and quantification of Ag+. *Rev. Mex. Fis.* **2000**, *46*, 132−134.

(13) (a) Berger, R. S.; Fu, J. L.; Smiles, K. A.; Turner, C. B.; Schnell, B. M.; Werchowski, K. M.; Lammers, K. M. The effects of minoxidil,

1% pyrithione zinc and a combination of both on hair density: a randomized controlled trial. *Br. J. Dermatol.* **2003**, *149*, 354−362. (b) Hosking, A.-M.; Juhasz, M.; Atanaskova Mesinkovska, N. Complementary and Alternative Treatments for Alopecia: A Comprehensive Review. *Skin Appendage Disord.* **2019**, *5*, 72−89.

(14) (a) Garcia-Orozco, I.; Lopez-Cortes, J. G.; Ortega-Alfaro, M. C.; Toscano, R. A.; Penieres-Carrillo, G.; Alvarez-Toledano, C. Synthesis, Characterization, and Tautomerism of Four Novel Copper(I) Complexes from 3-Hydroxy-3-(*p*-R-phenyl)-2-propenedithioic Acids. *Inorg. Chem.* **2004**, *43*, 8572−8576. (b) Garcia-Orozco, I.; Ortega-Alfaro, M. C.; Lopez-Cortes, J. G.; Toscano, R. A.; Alvarez-Toledano, C. Synthesis and Characterization of Novel Dinuclear Copper(I) Complexes. Dimerization of $[CuL(PPh_3)_2]$ (L = methyl 3-hydroxy-3-(*p*-R-phenyl)-2-propenedithioate). *Inorg. Chem.* **2006**, *45*, 1766−1773. (c) Saumweber, R.; Robl, C.; Weigand, W. Synthesis and coordination properties of amphiphilic 3-oxodithiocarboxylic esters. *Inorg. Chim. Acta* **1998**, *269*, 83−90. (d) Gompper, R.; Schaefer, H. Beitrage zur Chemie der Dithiocarbonsaureester und Ketenmer captale. *Chem. Ber.* **1967**, *100*, 591−604. (g) Dorange, G.; Guerchais, J. E. *Bull. Soc. Chim. Fr.* **1971**, 43.

(15) (a) Yadav, M. K.; Rajput, G.; Srivastava, K.; Singh, R. K.; Mishra, R.; Drew, M. G. B.; Singh, N. Anti-leishmanial activity of Ni(II), Pd(II) and Pt(II) A-oxodithioester complexes. *New J. Chem.* **2015**, *39*, 6358−6366. (b) Yadav, M. K.; Maurya, A. K.; Rajput, G.; Manar, K. K.; Vinayak, M.; Drew, M. G. B.; Singh, N. New planar trans-copper(II) β-dithioester chelate complexes: synthesis, characterization, anticancer activity and DNA-binding/cleavage studies. *J. Coord. Chem.* **2017**, *70*, 565−583. (c) Yadav, M. K.; Maurya, A. K.; Rajput, G.; Manar, K. K.; Vinayak, M.; Drew, M. G. B.; Singh, N. Synthesis, characterization, DNA binding and cleavage activity of homoleptic zinc(II) β-oxodithioester chelate complexes. *J. Coord. Chem.* **2017**, *70*, 3171−3185.

(16) (a) Xia, Q.-H.; Ge, H.-Q.; Ye, C.-P.; Liu, Z.-M.; Su, K.-X. Advances in Homogeneous and Heterogeneous Catalytic Asymmetric Epoxidation. *Chem. Rev.* **2005**, *105*, 1603−1662. (b) Mancheno, O. G.; Arrayas, R. G.; Carretero, J. C. Palladium Complexes of Chiral Planar 1-Phosphino-2-sulfenylferrocenes as Efficient Catalysts in Enantioselective Diels-Alder Reactions. *Organometallics* **2005**, *24*, 557−561. (c) Evans, D. A.; Michael, F. E.; Tedrow, J. S.; Campos, K. R. Application of Chiral Mixed Phosphorus/Sulfur Ligands to Enantioselective Rhodium-Catalyzed Dehydroamino Acid Hydrogenation and Ketone Hydrosilylation Processes. *J. Am. Chem. Soc.* **2003**, *125*, 3534−3543. (d) Mandimutsira, B. S.; Yamarik, J. L.; Brunold, T. C.; Gu, W.; Cramer, S. P.; Riordan, C. G. Dioxygen Activation by a Nickel Thioether Complex: Characterization of a $Ni^{III}_2(\mu\text{-}O)_2$ Core. *J. Am. Chem. Soc.* **2001**, *123*, 9194−9195. (e) McGuinness, D. S.; Wasserscheid, P.; Keim, W.; Morgan, D.; Dixon, J. T.; Bollmann, A.; Maumela, H.; Hess, F.; Englert, U. First Cr(III)-SNS Complexes and Their Use as Highly Efficient Catalysts for the Trimerization of Ethylene to 1-Hexene. *J. Am. Chem. Soc.* **2003**, *125*, 5272−5273. (f) Kumari, K.; Singh, A. S.; Manar, K. K.; Yadav, C. L.; Tiwari, V. K.; Drew, M. G. B.; Singh, N. Catalytic activity of new heteroleptic $[Cu(PPh_3)_2\text{-}(\beta\text{-oxodithioester})]$ complexes: click derived triazolyl glycoconjugates. *New J. Chem.* **2019**, *43*, 1166−1176.

(17) Yadav, C. L.; Rajput, G.; Manar, K. K.; Kumari, K.; Drew, M. G. B.; Singh, N. Cooperative metal-ligand influence on the formation of coordination polymers, and conducting and photophysical properties of Tl(I) β-oxodithioester complexes. *Dalton Trans.* **2018**, *47*, 16264−16278.

(18) Yadav, C. L.; Rajput, G.; Bisht, K. K.; Drew, M. G. B.; Singh, N. Spontaneous Resolution upon Crystallization and Preferential Induction of Chirality in a Discrete Tetrahedral Zinc(II) Complex Comprised of Achiral Precursors. *Inorg. Chem.* **2019**, *58*, 14449−14456.

(19) Rajput, G.; Yadav, M. K.; Drew, M. G. B.; Singh, N. Influence of the ligand frameworks on the coordination environment and properties of new phenylmercury(II) β-oxodithioester complexes. *Dalton Trans.* **2015**, *44*, 5909−5916.

(20) Furniss, B. S.; Hannaford, A. J.; Smith, P. W. G.; Tatchell, A. R. *Vogel's Textbook of Practical Organic Chemistry*, 5th ed.; Pearson: Harlow, 1989.

(21) Lee, A. W. M.; Chan, W. H.; Wong, H. C. One Pot Phase Transfer Synthesis of Trithiocarbonates from Carbon Bisulphide and Alkyl Halides. *Synth. Commun.* **1988**, *18*, 1531−1536.

(22) Frisch, M. J.; Trucks, G. W.; Schlegel, H. B.; Scuseria, G. E.; Robb, M. A.; Cheeseman, J. R.; Montgomery, J. A., Jr.; Vreven, T.; Kudin, K. N.; Burant, J. C.; Millam, J. M.; Iyengar, S. S.; Tomasi, J.; Barone, V.; Mennucci, B.; Cossi, M.; Scalmani, G.; Rega, N.; Petersson, G. A.; Nakatsuji, H.; Hada, M.; Ehara, M.; Toyota, K.; Fukuda, R.; Hasegawa, J.; Ishida, M.; Nakajima, T.; Honda, Y.; Kitao, O.; Nakai, H.; Klene, M.; Li, X.; Knox, J. E.; Hratchian, H. P.; Cross, J. B.; Bakken, V.; Adamo, C.; Jaramillo, J.; Gomperts, R.; Stratmann, R. E.; Yazyev, O.; Austin, A. J.; Cammi, R.; Pomelli, C.; Ochterski, J. W.; Ayala, P. Y.; Morokuma, K.; Voth, G. A.; Salvador, P.; Dannenberg, J. J.; Zakrzewski, V. G.; Dapprich, S.; Daniels, A. D.; Strain, M. C.; Farkas, O.; Malick, D. K.; Rabuck, A. D.; Raghavachari, K.; Foresman, J. B.; Ortiz, J. V.; Cui, Q.; Baboul, A. G.; Clifford, S.; Cioslowski, J.; Stefanov, B. B.; Liu, G.; Liashenko, A.; Piskorz, P.; Komaromi, L.; Martin, R. L.; Fox, D. J.; Keith, T.; Al-Laham, M. A.; Peng, C. Y.; Nanayakkara, A.; Challacombe, M.; Gill, P. M. W.; Johnson, B.; Chen, W.; Wong, M. W.; Gonzalez, C.; Pople, J. A. *Gaussian 03, Rev. C.02*; Gaussian, Inc.: Wallingford, CT, 2004.

(23) *CrysAlis CCD, RED, version 1.711.13*; Oxford Diffraction Poland Sp: 1995−2003.

(24) *Smart & SAINT Software Reference Manuals, Version 6.45*; Bruker Analytical X-ray Systems, Inc., Madison, WI, 2003.

(25) Sheldrick, G. M. *SHELXS-97*, A short history of SHELX. *Acta Crystallogr., Sect. A: Found. Crystallogr.* **2008**, *A64*, 112−122.

(26) Sheldrick, G. M. SHELXL2016−6. *Acta Crystallogr.* **2015**, *C71*, 3−8.

(27) (a) Brandenburg, K. *DIAMOND*; Crystal Impact GbR: Bonn, Germany, 1999. (b) Macrae, C. F.; Bruno, I. J.; Chisholm, J. A.; Edgington, P. R.; McCabe, P.; Pidcock, E.; Rodriguez-Monge, L.; Taylor, R.; van de Streek, J.; Wood, P. A. *Mercury CSD 2.0* − New Features for the Visualization and Investigation of Crystal Structures. *J. Appl. Crystallogr.* **2008**, *41*, 466−470.

(28) (a) Bisht, K. K.; Suresh, E. Spontaneous Resolution to Absolute Chiral Induction: Pseudo-Kagomé Type Homochiral Zn(II)/Co(II) Coordination Polymers with Achiral Precursors. *J. Am. Chem. Soc.* **2013**, *135*, 15690−15693. (b) Janiak, C.; Chamayou, A.-C.; Royhan Uddin, A. K. M.; Uddin, M.; Hagen, K. S.; Enamullah, M. Polymorphs, enantiomorphs, chirality and helicity in [Rh{N, O}(η4-cod)] complexes with {N, O} = salicylaldiminato Schiff base or aminocarboxylato ligands. *Dalton Trans.* **2009**, 3698−3709.

(29) (a) Morales, A. E.; Mora, E. S.; Pal, U. Use of diffuse reflectance spectroscopy for optical characterization of un-supported nanostructures. *Revista Mexicana de Física S* **2007**, *53*, 18−22. (b) Rajput, G.; Yadav, M. K.; Drew, M. G. B.; Singh, N. Impact of Ligand Framework on the Crystal Structures and Luminescent Properties of Cu(I) and Ag(I) Clusters and a Coordination Polymer Derived from Thiolate/Iodide/dppm Ligands. *Inorg. Chem.* **2015**, *54*, 2572−2579.

(30) Tauc, J.; Grigorovici, R.; Vancu, A. Optical Properties and Electronic Structure of Amorphous Germanium. *Phys. Status Solidi B* **1966**, *15*, 627−637.

(31) (a) Zhao, X.; Zhang, S.; Yan, J.; Li, L.; Wu, G.; Shi, W.; Yang, G.; Guan, N.; Cheng, P. Polyoxometalate-Based Metal−Organic Frameworks as Visible-Light-Induced Photocatalysts. *Inorg. Chem.* **2018**, *57*, 5030−5037. (b) Liu, Y.; Wei, F.; Yeo, S. N.; Lee, F. M.; Kloc, C.; Yan, Q.; Hng, H. H.; Ma, J.; Zhang, Q. Synthesis, Crystal Structure, and Optical Properties of a Three- Dimensional Quaternary Hg-In-S-Cl Chalcohalide: $Hg_7InS_6Cl_5$. *Inorg. Chem.* **2012**, *51*, 4414−4416. (c) Okubo, T.; Anma, H.; Tanaka, N.; Himoto, K.; Seki, S.; Saeki, A.; Maekawa, M.; Karuda-Sowa, T. *Chem. Commun.* **2013**, *49*, 4316−4318.

(32) (a) Chai, J.; Lai, C. S.; Yan, J.; Tiekink, E. R. T. Polymeric [bis(N, N-diethyldithiocarbamato) (trans-1,2-bis(4-pyridyl)-

ethylene)cadmium(II)]. *Appl. Organomet. Chem.* **2003**, *17*, 249−250. (b) Zhu, L.-N.; Deng, Z.-P.; Ng, S. W.; Huo, L.-H.; Gao, S. Cd(II) coordination polymers constructed from bis(pyridyl) ligand with asymmetric spacer in chelating mode and diverse organic dicarboxylates: syntheses, structural evolutions and properties. *Dalton Trans.* **2019**, *48*, 7589−7601.

(33) (a) Yeo, C. I.; Halim, S. N. A.; Ng, S. W.; Tan, S. L.; Schpector, J. Z.; Ferreira, M. A. B.; Tiekink, E. R. T. Investigation of putative arene-C−H···π(quasi-chelate ring) interactions in copper(i) crystal structures. *Chem. Commun.* **2014**, *50*, 5984−5986. (b) Tiekink, E. R. T.; Schpector, J. Z. Emerging supramolecular synthons: C−H···π-(chelate) interactions in metal bis(1,1-dithiolates). *Chem. Commun.* **2011**, *47*, 6623−6625.

(34) Tietze, L. F. Domino Reactions in Organic Synthesis. *Chem. Rev.* **1996**, *96*, 115−136.

(35) Freeman, F. Properties and Reactions of Ylidenemalononitriles. *Chem. Rev.* **1980**, *80*, 329−350.

(36) Pande, A.; Ganesan, K.; Jain, A. K.; Gupta, P. K.; Malhotra, R. C. A Novel Eco-Friendly Process for the Synthesis of 2-Chlorobenzylidenemalononitrile and ITS Analogues Using Water As a Solvent. *Org. Process Res. Dev.* **2005**, *9*, 133−136.

(37) (a) Jensen, A. A.; Erichsen, M. N.; Nielsen, C. W.; Stensbøl, T. B.; Kehler, J.; Bunch, L. Discovery of the First Selective Inhibitor of Excitatory Amino Acid Transporter Subtype 1. *J. Med. Chem.* **2009**, *52*, 912−915. (b) Mansouri, K.; Khodarahmi, R.; Foroumadi, A.; Mostafaie, A.; Motlagh, H. M. Anti-angiogenic/proliferative behavior of a '-4-aryl-4H-chromene" on blood vessel's endothelial cells: A possible evidence on dual '-anti-tumor" activity. *Med. Chem. Res.* **2011**, *20*, 920−929. (c) Fallah-Tafti, A.; Tiwari, R.; Shirazi, A. N.; Akbarzadeh, T.; Mandal, D.; Shafiee, A.; Parang, K.; Foroumadi, A. 4-Aryl-4H-Chromene-3-Carbonitrile Derivatives: Evaluation of Src Kinase Inhibitory and Anticancer Activities. *Med. Chem.* **2011**, *7*, 466−472. (d) Fernández-Bachiller, M. I.; Pérez, C. N.; Monjas, L.; Rademann, J. R.; Rodríguez-Franco, M. I. New Tacrine−4-Oxo-4*H*-chromene Hybrids as Multifunctional Agents for the Treatment of Alzheimer's Disease, with Cholinergic, Antioxidant, and β-Amyloid-Reducing Properties. *J. Med. Chem.* **2012**, *55*, 1303−1317.

(38) (a) Sharma, P.; Gupta, M.; Kant, R.; Gupta, V. K. One-pot synthesis of various 2-amino-4*H*-chromene derivatives using a highly active supported ionic liquid catalyst. *RSC Adv.* **2016**, *6*, 32052−32059. (b) Majumdar, N.; Paul, N. D.; Mandal, S.; de Bruin, B.; Wulff, W. D. Catalytic Synthesis of 2H-Chromenes. *ACS Catal.* **2015**, *5*, 2329−2366.

https://dx.doi.org/10.1021/acs.inorgchem.0c01195
Inorg. Chem. XXXX, XXX, XXX−XXX